Front. Phys. China, 2010, 5(3): 220–244
DOI 10.1007/s11467-010-0100-0

REVIEW ARTICLE

Ultrafast optical switching in Kerr nonlinear photonic crystals

Ye LIU (刘晔), **Fei QIN** (秦飞), **Fei ZHOU** (周飞), **Qing-bo MENG** (孟庆波), **Dao-zhong ZHANG** (张道中), **Zhi-yuan LI** (李志远)†

Beijing National Laboratory of Condensed Matter Physics, Institute of Physics, Chinese Academy of Sciences, P. O. Box 603, Beijing 100190, China
E-mail: lizy@aphy.iphy.ac.cn

Nonlinear photonic crystals made from polystyrene materials that have Kerr nonlinearity can exhibit ultrafast optical switching when the samples are pumped by ultrashort optical pulses with high intensity due to the change of the refractive index of polystyrene and subsequent shift of the band gap edge or defect state resonant frequency. Polystyrene has a large Kerr nonlinear susceptibility and almost instantaneous response to pump light, making it suitable for the realization of ultrafast optical switching with a response time as short as a few femtoseconds. In this paper, we review our experimental progress on the continual improvement of all-optical switching speed in two-dimensional and three-dimensional polystyrene nonlinear photonic crystals in the past years. Several relevant issues are discussed and analyzed, including different mechanisms for all-optical switching, preparation of nonlinear photonic crystal samples by means of microfabrication and self-assembly techniques, characterization of optical switching performance by means of femtosecond pump-probe technique, and different ways to lower the pump power of optical switching to facilitate practical applications in optical information processing. Finally, a brief summary and a perspective of future work are provided.

Keywords nonlinear photonic crystal, all-optical switching, Kerr nonlinearity, femtosecond pump–probe technique, photonic crystal cavities

PACS numbers 42.70.Qs, 42.65.Pc, 42.65.Hw

Contents

1 Introduction

In the past half century information technology has made great progress and has significantly shaped the way we live in our society. This has been possible due to the prosperity of the microelectronics industry for handling

digital information data and the optical fiber communication industry for transporting information at high speeds, huge amounts, and long distances. It is now hard to imagine life without a computer, mobile phone, and Internet. Nonetheless, the ever-increasing demand for faster information transport and processing capabilities has never gone to an end. Demand on higher-level information technology in our data-hungry society has driven enormous progress in the silicon microelectronics industry and we have witnessed a continuous progression towards smaller, faster, and more efficient electronic devices in the past, current, and future days. Nonetheless, the downscaling of the size of these devices has also brought about a wide variety of fundamental and technological challenges. Currently, two of the most daunting problems preventing significant increases in the microelectronic processor speed are thermal and signal delay issues associated with electronic interconnection. Optical interconnects, on the other hand, possess an almost unimaginably large data carrying capacity, and may offer interesting new solutions for circumventing these problems. Photons are good carriers for information and energy because they have much faster transfer speed, better parallel degree, and more capabilities of frequency carrier than electrons.

In this context, more and more attention has been drawn to the realization of large-scale ultrasmall all-optical or optoelectronic integrated circuits that allow fast information processing and easy coupling and connection with the microelectronic circuit. Several schemes have been proposed and seriously explored and examined, including those based on photonic crystal devices [1–3] and plasmonic devices made from metal nanostructures [4, 5], which are able to realize optical devices on the wavelength scale of light signals. Great efforts have been extensively made not only in the design and realization of different types of high performance optical functional elements that are necessary for constructing an integrated optical circuit, but also in the development of a new chip-scale device technology that can help information transport and connection between nanoscale devices at optical frequencies and bridge the gap between the world of nanoscale electronics and microscale photonics.

In the way to pursue an all-optical integrated circuit, different composite functional elements have been designed, optimized, and brought into reality by state-of-the-art microfabrication technologies on silicon-on-insulator (SOI) or other III–V semiconductors platform. These technologies include electron-beam lithography, focused ion-beam (FIB) lithography, and X-ray lithography, in combination with wet and dry etching techniques. Two categories of optical devices are considered: the passive devices that include waveguides, cavities, filters, waveguide bends and splitters, interferometers, and so on, and active devices that include nanolasers, modulators, optical switches, photodetectors, and so on. To bring these elements and devices into practice and more importantly into large-scale integration for useful optical signal processing applications, several fundamental and technological obstacles need to be overcome. The first is the idea and scheme to design high performance devices, mainly through large scale numerical simulations and optimizations. The second is use of high accuracy microfabrication technologies, which is now pretty mature due to the long history of the microelectronics industry. The third is to find high performance materials based on which these devices are realized. The ordinary semiconductors cannot satisfy all special demands for different signal processing functionalities. For instance, although silicon photonic crystals have large photonic band gaps due to the large refractive index of silicon ($n = 3.4$) around the telecommunication wavelength of 1.55 μm and allows for building of many useful devices based on defect states, silicon is not a good material for photoemission that promises for nanolasers. Another example is that all semiconductors do not have large enough optical nonlinearity, so it is hard to make practical high speed optical switches and modulators based on microscale photonic crystal devices. It is thus very important to develop suitable materials that are compatible with semiconductor photonic crystal devices.

All-optical switching is an essential component in all-optical networks. Compared with the traditional electro-optical switching, all-optical switching has the obvious advantage of ultra-fast time response, which meets the need of high-speed information processing. Many researchers have concentrated on this aspect for a long time. Several materials, ranging from dielectrics to semiconductors and organics, have been investigated to characterize their linear and nonlinear properties for all-optical switching. Friberg *et al.* reported the first demonstration of a nonlinear dual-core fiber coupler switch capable of substantial complete all-optical switching at subpicosecond rates [6]. Almeida *et al.* realized an all-optical switching on a silicon chip by the structure of ring resonator [7, 8]. Sasaki *et al.* proposed an all-optical switching in a composite thin film of silver and polymer matrix containing photochromic dye [9, 10]. However, there are still several main challenges for the practical application of all-optical switching: very high pump intensity, low switch contrast, and the response time limits set by the materials or the physical principles themselves. Therefore, searching for nonlinear materials that possess a larger third-order (namely, Kerr) nonlinear susceptibility ($\chi^{(3)}$) and designing more suitable structures that can effectively enhance the inner field at the nonlinear areas are two effective ways to improve the performance of all-optical switching.

Compared with the traditional semiconductor mate-

rials, such as silicon, InP, or GaAs, conjugated organic molecules and polymers [11, 12] possess a relatively large third-order nonlinear susceptibility and femtosecond response time, which are of great importance to the realization of all-optical switching. Note that the third-order optical nonlinear susceptibility is on the order of 10^{-12} cm^2/W for usual conjugated organic molecules and 10^{-14} cm^2/W for traditional semiconductor materials. Moreover, by introducing dye molecules [13–15] or gold nanoparticles [16] into the polymer thin films, the third-order nonlinear susceptibility will become even larger.

On the other hand, the photonic crystal, which has periodic dielectric or metal-dielectric arrays in one-, two- or three-dimensional space, is a very good arrangement to provide the high field enhancement effect in the nonlinear optics areas. The photonic crystal, first proposed by Yablonovitch [17] and John [18] in 1987, can control the propagation of electromagnetic waves in the same way as periodic potential in a semiconductor crystal affects the electron motion by defining allowed and forbidden electronic energy bands. Because of coherent Bragg scattering by the periodic arrays, the photonic crystal has the property of band gap effect [19–25], and light waves with the frequencies located within the band gap are forbidden to propagate. When a disorder (such as line or point defect) is introduced into the periodic structures artificially, there will be localized defect modes in the band gap frequency regions [26–34]. Because of the combination of these two effects, photonic crystals have found potential applications in a wide variety of areas such as inhibition of spontaneous emission [35–39], high-reflecting omnidirectional mirrors [40–43], low-loss waveguides [44–48], photonic crystal fibers [49–52], optical filters [32, 53–55], diodes [56, 57], all-optical switching [58–63] and so on.

By introducing nonlinear optical materials into photonic crystal structures, the optical properties can be tuned by an external drive, such as a strong pump laser. This tunable property is important for all-optical switching or modulators. Nowadays, many researches of all-optical switching have turned to nonlinear photonic crystal structures, which involve Kerr nonlinear materials in the structure. In theory, Fan *et al.* proposed an analytic theory to study the switching dynamics in photonic crystal microcavities [64]. Soljacic *et al.* investigated properties of hybrid systems of photonic crystal microcavities incorporating a highly nonlinear ultraslow light medium, and found that such systems can enable ultrafast nonlinear all-optical switching at ultralow (even single photon) energy levels [65]. In experiment, Tanabe et al. reported an all-optical switching in the telecommunication band with extremely low switching energy (a few 100 fJ), high switching contrast (about 10 dB), and high speed (about 50 ps) on the silicon chip by using photonic crystal nanocavities [66]. Hu *et al.* reported ultrafast and low-power photonic crystal all-optical switching based on strong optical nonlinearity enhancement due to excited-state inter-electron transfer [15]. The switching operation power is reduced by four orders of magnitude, and the ultrafast response time is on the order of one picosecond.

It is the aim of this review paper to discuss ultrafast optical switching based on nonlinear photonic crystals. Several aspects of basic physical and material science problems will be addressed. We illustrate the fundamental physical principles of all-optical switching in nonlinear photonic crystals and highlight the recent experimental progress that we have made to continually increase the switching speed to its limit. The arrangement of this article is as follows. In Section 2 we present the fundamental physical principle of all-optical switching in nonlinear photonic crystals with several different operation routines. In Section 3 we discuss several materials science schemes to realize nonlinear photonic crystal structures for all-optical switching application. The detailed experimental preparations, arrangements and measurements in two- and three-dimensional nonlinear photonic crystal all-optical switching are shown in Sections 4 and 5, respectively. In Section 6 we further discuss ways towards low-pump-power and high-switching-contrast all-optical switching. Finally, we summarize this review in Section 7.

2 Principles of all-optical switching in nonlinear photonic crystals

Generally speaking, all-optical switching in nonlinear photonic crystals can be classified into two kinds. In the first kind, the switching exploits the nonlinearity of the material by controlling the intensity of the input signal, and this utilizes a sort of self-switching effect where the input pulse will trigger optical switching by itself. In the second kind, the nonlinearity is exploited by launching a control beam to trigger optical switching for the input signal which can maintain a relative low level of intensity. Nonlinear photonic crystal provides new mechanisms to realize all-optical switching based on different nonlinear effects. In the following, several mechanisms that are usually used in photonic crystal structures are analyzed, which include photonic band gap edge shift, defect mode shift, optical bistability effect, and two-photon absorption effect.

2.1 Band gap edge and defect mode shift

According to the basic electromagnetic theory of photonic crystals, the band gap is strongly dependent on the refractive index of each composite material. Therefore, for a nonlinear photonic crystal with a composite material exhibiting Kerr nonlinearity, the refractive in-

dex will change dynamically under the incident high-intensity pump beam, which will lead to the shift of the photon band gap [67–69] [see the schematic of Fig. 1(a)]. When the signal light is just located at the band gap edge, its transmission energy will change dynamically with respect to the pump beam as the signal light either sees the pass band with high transmissivity under no pump light or the band gap with low transmissivity under pump light. The contrast in the transmission signal intensity will realize the "on" and "off" state of an optical switching. More interestingly, because the optical switching is driven by the external pump light, the major properties of the switching, which is the response speed and switching contrast, can be well controlled by the intensity and pulse duration of the pump light. Suppose that the nonlinear material has a very fast (say, almost instantaneous) optical response to the driven light, the response time of the switching should be on the order of the duration time of the pump light pulse. This means that it is possible to utilize state-of-the-art ultrashort pulse laser technique, in particular the femtosecond laser technique, to realize a super-fast switching speed (down to a few femtoseconds) that is several orders of magnitude larger than the traditional optoelectronic switching (tens of picoseconds).

There is another unique property for photonic crystals–existence localized defect modes that are easy to engineer and control [30, 70, 71]. When a defect is intentionally introduced into the periodic arrays in an appropriate way, a high transmission state will appear in the band gap with a sharp and narrow resonance peak, and this corresponds to a defect mode. The defect state will also shift with the change of refractive index. Similar to the situation of band gap edge shift, the shift of defect state can also be exploited as a controllable optical switching under external pump light. Such a picture is depicted in Fig. 1(b). By suitable designing, the defect mode shift can be made to be much more sensitive than the band gap edge shift upon a tiny change of refractive index. This may be very useful to reduce the pump power of all-optical switching. More details will be discussed in Section 6.

2.2 Optical bistability effect

Optical bistability is an important effect for many nonlinear optical devices. When this effect is combined with photonic crystals, it shows promising prospects in optical switching. A system with optical bistability has two stable resonant transmission states, dependent on the input and the history, and this feature can be utilized to serve as optical switching, which basically belongs to the category of self-switching scheme. Two factors should be satisfied in the nonlinear system: nonlinear interaction between the nonlinear material and input optical field, and the feedback process. Figure 2 shows the typical output–input curve of an optical bistability system. When the input intensity is zero, the wavelength of the input light ($\lambda_{\rm I}$) is longer than the resonant wavelength of the nonlinear system ($\lambda_{\rm R}$), that is $\lambda_{\rm I} > \lambda_{\rm R}$, which is shown in Fig. 2(a). For simplicity, we suppose the third-order nonlinear coefficient of the system is $n_2 > 0$. The resonant condition of the system is $(n_0 + n_2)I = k\lambda_{\rm R}$, where n_0 is the linear refractive index, I is the local light intensity at the nonlinear material, and k is an integer. When increasing the intensity of the input light, the resonant intensity I is increased, so $\lambda_{\rm R}$ will shift to a longer wavelength ($n_2 > 0$), and it is closer to the input wavelength $\lambda_{\rm I}$, which will further increase the resonant intensity (with I increasing). In this process, the positive feedback happens, following the procedure as:

$$I_{\rm in} \uparrow \rightarrow \lambda_{\rm R} \uparrow \rightarrow (\lambda_{\rm I} - \lambda_{\rm R}) \downarrow$$

When the input intensity increases to a certain value, $I_{\rm M}$, a sudden increase of output intensity will happen, and the output intensity jumps from the lower branch to the higher branch, which corresponds to the resonance between the nonlinear system and the input light. After this jump, when the input intensity further increases, the resonant wavelength $\lambda_{\rm R}$ still shifts to the longer wavelength, which will be away from the input wavelength $\lambda_{\rm I}$, and the negative feedback happens. On the other hand, when the input intensity is at the high branch initially, the opposite process will happen. Simply speaking, when the input light is weak, the output is low, and this cor-

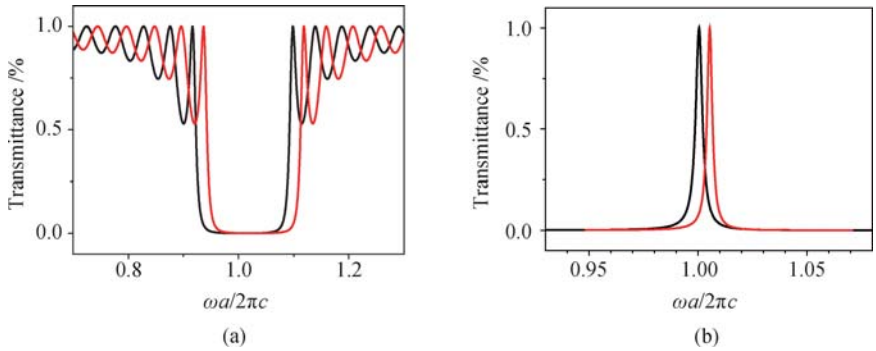

Fig. 1 Schematic picture of optical switching utilizing **(a)** the band gap edge shift and **(b)** defect mode shift under the high-intensity pump light upon a Kerr nonlinear photonic crystal. Black and red curves correspond to the transmission spectrum before and after external pump light.

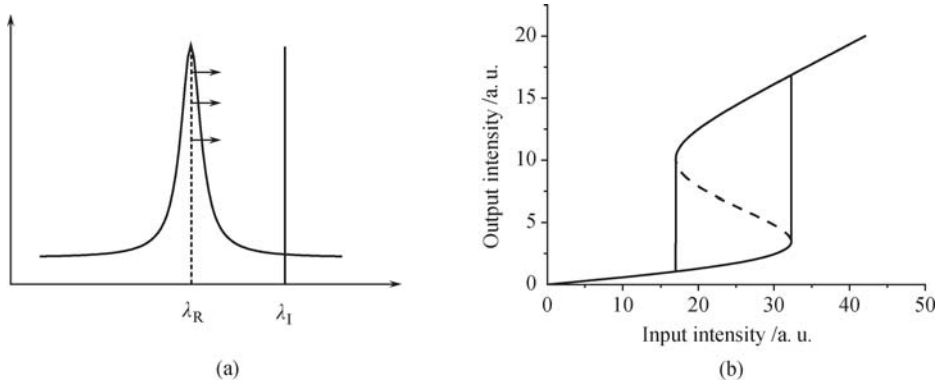

Fig. 2 **(a)** Schematic to show the principle of optical bistability, and **(b)** the input-output curve of optical bistability. There are two steady states, which operate at lower and higher beam intensities. The dashed line corresponds to an unstable state of the system.

responds to the "off" state. On the contrary, when the input light is strong, the output is sharply and nonlinearly increased, and this corresponds to the "on" state. The output signal intensity for the "on" state and the "off" state has a sharp contrast due to nonlinear bistability. It can be seen clearly that the input light pulse itself is enough to perform optical switching functionalities merely by nonlinear coupling with the resonant state.

In a photonic crystal with Kerr nonlinearity, a resonant cavity can serve as the basis for optical bistability. Nonlinear coupling between the input light, which might transport through a single-mode photonic crystal waveguide, and the cavity will lead to optical bistability following the same physical procedure as described above in Fig. 2. All-optical switching in nonlinear photonic crystals based on optical bistability has been studied theoretically [64, 70, 72–77]. A great advantage for photonic crystal cavity is that a high quality (Q) factor nanocavity can be designed at will and realized experimentally, and this can greatly lower the input light power level that is sufficient to ignite considerable optical bistability. Nonetheless, due to the difficulty in creating a nonlinear photonic crystal with strong enough Kerr nonlinear coefficient and accessible infrared signals with high enough power level at nanoscale, the concept of optical bistability switching in photonic crystals has yet to be demonstrated experimentally even with the help of signal enhancement in high-Q resonant cavity.

2.3 Two-photon absorption effect

Two-photon absorption effect [78–80] can also be used to realize all-optical switching in photonic crystals [81]. The usual materials that possess a large two-photon absorption cross section are mostly semiconductors, such as silicon, GaAs, and some organic polymers. This makes it possible to realize two-photon absorption optical switching in semiconductor photonic crystals with good band gap and defect mode performance. One way to achieve ultrafast optical switching in silicon is by exploiting its ultrafast nonlinear optical properties. The idea is to increase the density of free carriers in silicon and enhance its refractive index by using an intense ultrashort laser pulse at the electronic band-edge of silicon. Optically excited electrons and holes induce ultrafast alteration of refractive index in silicon, causing a shift in the optical Bragg diffraction of the photonic crystal from its original position [82] or a shift in the resonant frequency of a photonic crystal microcavity. Nowadays, many researches have demonstrated the properties of all-optical switching with two-photon absorption in silicon [81, 83, 84]. Nonetheless, the free-carrier absorption effect has a limit in the response time, which is on the order of sub-nanosecond. This makes it difficult to pursue much faster optical switching speed that is well below the subpicosecond level by this two-photon absorption scheme.

The optical bistability scheme and two-photon absorption scheme rely merely on the input light signal to generate nonlinear optical effect that is sufficiently strong to induce a jump between "on" and "off" state of photonic crystal resonant modes. This requires either strong Kerr optical nonlinearity or large two-photon absorption cross sections. This has brought about a serious problem in the material part. Because light signal transporting in a photonic crystal integrated circuit is usually weak due to low-efficiency injection of light power from a single-mode fiber into the photonic crystal chip, it is currently difficult to trigger an observable self-switching effect in the nanoscale system made from usual semiconductor materials.

Taking this difficulty into full account, in the past several years our work has been focused on the design, realization, and characterization of ultrafast all-optical switching in nonlinear photonic crystals under external pump light of a femtosecond laser pulse with very high peak power level. We have demonstrated successfully efficient optical switching based on band gap edge shift or defect state shift in two- and three-dimensional nonlinear photonic crystals with a response time scaled down

to a few femtoseconds. At the same time, different approaches have been exploited to lower down the pump light level and increase the effective nonlinear coefficient. We have found that a compromise might be needed between response speed and power level in practical applications.

3 Nonlinear materials for all-optical switching

The above discussions on the physical principles for different schemes of optical switching in nonlinear photonic crystals have clearly indicated the importance of appropriate nonlinear materials for realizing high performance all-optical switching. Three main types of nonlinear materials have been extensively used in tunable photonic crystals: dielectrics, semiconductors, and polymer materials.

3.1 Dielectric materials

Most of the nonlinear dielectric materials are ferroelectric inorganic crystals, such as the potassium dideuterium phosphate (KDP) crystal, the lithium niobate ($LiNbO_3$) crystal, barium titanate ($BaTiO_3$) crystal and so on. These ferroelectric materials exhibit significant photorefractive effect that allows the crystal to change its refractive index under illumination of external light wave. Although the crystal growth technology for these materials has been highly developed and their optical nonlinear susceptibilities are sufficient for most current photonic applications, they have some disadvantages in all-optical switching applications. One feature is the constraint of working with only single crystalline materials and another is the relatively slow optical switching time, which is in the millisecond range.

Another attention on nonlinear dielectric materials is paid to silica fibers [51, 85, 86]. In silica fibers, the third-order nonlinearity is dominant as the second-order nonlinearity disappears because of the symmetry in the microscopic atomic level. Although the third-order nonlinear susceptibility of silica fibers is very small, the nonlinear effects, such as self-phase modulation (SPM), cross-phase modulation (XPM), and third-harmonic generation, are still obvious due to the very long interaction length. Petropoulos *et al.* reported all-optical switching based on the SPM effect of a highly nonlinear holey fiber made from pure silica [87], and Sharping *et al.* proposed an all-optical switching based on the XPM effect of photonic crystal fibers [88]. Nowadays, the photonic crystal fiber is still an important material to realize all-optical switching. As silica fibers mainly depend on their long distance to accumulate and amplify Kerr nonlinearity, they are not suitable for the creation of microscale/nanoscale all-optical switching devices that will be placed in the background of an integrated optical circuit.

3.2 Semiconductor materials

Semiconductor materials have played a great role in the microelectronic technologies, and they are now also a very good platform for creating photonic crystal integrated devices and chips because of their relatively large refractive index in the telecommunication wavelength. Nowadays, all-optical switching and modulators have been demonstrated with III–V compound semiconductors [89, 90]. For silicon, a more popular and important semiconductor material, it is harder to achieve the same performances of all-optical switching due to its relatively weak optical nonlinearity and bad optoelectronic properties. Despite the difficulties, more and more efforts have been made on the silicon or silicon-on-insulator (SOI) structures [7, 82, 91, 92] in order to realize all-optical switching on silicon photonic crystal structures.

The basic nonlinear effect on semiconductor materials is the two-photon absorption, as has been discussed in Section 2.3. As a result, the speed of these all-optical switches is limited by the effective carrier relaxation time, whose value is sub-nanoseconds for silicon microring cavities [7] and about 100 ps for line defect photonic crystal nanocavities [66]. The relaxation time can be shortened by ion implanted semiconductors, which allows for a faster switching recovery time for photonic crystal optical switching. Recently, Tanabe *et al.* reported an all-optical switching with the response time of 70 ps using ion-implanted silicon photonic crystal nanocavities [93]. Further downscaling of the optical switching response time will encounter enormous difficulties.

3.3 Polymer materials

Because of the development of synthetic, physical and theoretical chemistry, organic polymer materials have attracted much attention. Organic polymer materials are of major interest because of their relatively low cost, ease of fabrication and integration into devices, higher laser damage threshold, fast nonlinear optical response time, and off-resonance nonlinear optical susceptibilities comparable to or exceeding those of ferroelectric inorganic crystals [11]. In the field of photonic crystal all-optical switching, the widespread nonlinear polymer materials include liquid crystal, polystyrene, polymethyl methacrylate (PMMA), and polyphenylene vinylene (PPV). An earlier tunable photonic crystal in experiment [94] primarily focused on electro–optic and thermo–optic band edge tuning via infiltrated liquid crystals since Busch and John proposed the concept of tunable photonic crystal by means of infiltrating liquid crystal into the void regions of an inverse opal photonic

crystal structure [95]. However, the molecular reorientation processes responsible for changes in the refractive index of liquid crystal typically occur in a time scale ranging from milliseconds to seconds, and this strictly prohibits rapid band edge tuning. In regard to obtaining an ultrafast response speed, polystyrene [15, 58, 96], PMMA, and PPV have received many considerations due to the femtosecond response time and relatively large third-order nonlinear susceptibility in these polymer materials.

In addition to the aforementioned three types of nonlinear materials, there are still some new artificial materials that are exploited to realize all-optical switching. These include metal materials with surface plasma effect [97] and quantum dot [98] or quantum well materials with optical tunability through nonlinearity.

In the past several years, we have carried out a series of experiments on all-optical switching in photonic crystal structures made from the nonlinear material of polystyrene. We have made extensive efforts to continually improve the optical switching response time to its limit. In 2003, our first experiment [99] was demonstrated in an organic three-dimensional polystyrene opal photonic crystal structure, whose response time is several picoseconds. However, the transmission contrast, which is an important evaluation index for optical switching, is as low as 8% under the peak intensity of a pump laser of 14.4 GW/cm^2. With improvements on the quality of the photonic crystal sample, the band gap edge becomes steeper, which reduces the pump intensity and increases the transmission contrast. In 2005, we realized all-optical switching with the response time of 10 ps in two-dimensional polystyrene photonic crystal structures, which were based on the principle of band gap edge shift [58] and defect mode shift [100], respectively. The transmission contrast was as high as 65%. We also realized all-optical switching [96] in three-dimensional polystyrene opal structure in the same year, whose response time was as short as 120 fs, and the contrast was about 45% under the pump intensity of 27.5 GW/cm^2. An all-optical switching with 20 fs response time was then demonstrated in a two-dimensional polystyrene photonic crystal in 2006 [101]. In 2009, we fulfilled an all-optical switching of 10 fs [102] in a three-dimensional polystyrene opal nonlinear photonic crystal system. In Sections 4 and 5, we will review our progress in all-optical switching experiments.

4 All-optical switching in two-dimensional nonlinear photonic crystals

Since the basic physical phenomenon of photonic crystals is based on Bragg scattering in periodic lattice structures, the repeating regions of high and low dielectric constants have to be of the same length scale as half the wavelength of electromagnetic waves. So for the visible or infrared wave, the length scale of scattering units is on the order of 100 nm, which brings a major challenge for the fabrication of two- and three-dimensional photonic crystal structures. Nowadays, with the rising development of semiconductor technology, micro-fabrication technology and other micro/nano manipulation and characterization technologies, the study of two-dimensional photonic crystals has been focused on photonic crystal slabs. Photonic crystal slabs are two-dimensional photonic crystals "etched" into slabs of semiconductors or other substrates, where the two-dimensional band gap confines light in the parallel plane of the slab and the total internal reflection confines light within the slab. Our two-dimensional experiments are based on polystyrene photonic crystal slabs. In the following, we review our experimental details in two-dimensional structures, including the fabrication of photonic crystals, the experimental arrangements and the measured results of photonic crystal all-optical switching.

4.1 Preparation of two-dimensional polystyrene photonic crystals

In the two-dimensional photonic crystal experiment, we use polystyrene powder with normal molecular weight of 8 million (Fluka Chemie Company, Switzerland). First, the polystyrene powder is dissolved in toluene with a weight ratio of about 1:100. The spin coating method [103], which is the preferred method for the application of thin, uniform films to flat substrates, is then used to fabricate a thin film slab of polystyrene on a quartz substrate, which is pre-cleaned carefully. The thickness of the thin film is about 300 nm, which is measured by a surface profiler (Model Dektek 8, DI Company, USA). Changing the concentration of the polystyrene toluene solution, or changing the rotation speed during the spin coating process, the thickness of the thin film will be changed. We can select optimized experiment conditions as desired. Finally, a focused ion beam etching (FIB) system (Model DB235, FEI Company, USA) is employed to prepare the periodical patterns of the two-dimensional photonic crystal. Before etching the periodical patterns, a thin gold layer with thickness of about 15 nm is sputtered onto the surface of the polystyrene film, which is used to make up for the weak electrical conductivity of polystyrene. After the etching process, the thin gold layer is wiped off by the potassium iodide (KI) solution where the weight ratio of iodine (I_2), potassium iodide and distilled water is 1:1:4. In addition, because the required periodical patterns are much larger than the area that we can finish once, (the required patterned area is about, 3 μm × 100 μm while the area that we can etch

once by FIB is about 10 μm × 10 μm) the multiple screen joint technology is used during the process of etching by FIB. By this method, good quality photonic crystal samples are fabricated. The scanning electron microscopy (SEM) images of developed photonic crystal samples are depicted later in Figures 4, 8 and 10.

4.2 Experimental measurement system

In this subsection, the basic experimental setup for characterizing the performances of all-optical switching in a two-dimensional nonlinear photonic crystal is presented. In order to introduce the incident light into our photonic crystal thin film structures, three major coupling techniques that are widely used in two-dimensional photonic crystals can be used: the prism coupling, fiber coupling, and the grating coupling, respectively. Prism coupling [58, 104] is a traditional but effective method to realize coupling between the incident light and the optical thin film. It is based on the principle of evanescent field coupling. The incident light is totally reflected at the prism base, and under certain conditions [105], light energy can be transferred into the film by optical tunneling. This method is very simple, easy to operate, and it is suitable for photonic crystal structures with a relatively large area.

In two-dimensional silicon-based photonic crystals, the small mode profiles and complex optical phase within the periodic structures make it difficult to use the conventional direct coupling from free-space beams or through prism-based techniques to inject light signals into the photonic crystal. For example, in structures of high vertical index contrast, such as silicon-on-insulator or GaAs–AlO_x, light is strongly confined in a thin high refractive index layer of a few hundred nanometers and coupling light into these waveguides becomes a serious problem. To overcome this obstacle, a fiber edge-coupling technique [106] is developed to realize efficient input and output connection of light signals with the microstructure. To further improve the coupling efficiency from fiber to photonic crystal waveguides or cavities, a novel fiber taper coupling technique based on the evanescent field theory is proposed [107–109]. However, high insertion loss between the fiber and the microstructures and the positioning instability are still main problems that will affect the coupling efficiency greatly. Grating coupling [110], an out-of-plane coupling technique between a standard single-mode fiber and a waveguide, is proposed to tackle these problems [111]. The grating coupling approach has some major advantages. There is no need for a cleaved facet; light can be coupled in and out everywhere on the chip; it is suitable for low loss and broadband operation, and the coupling efficiency can be improved. Thus, the technique has attracted much attention [112–114].

In our experiments, the prism coupling method is used to realize the input and output of polystyrene thin films. The pump–probe technique is used to measure the ultrafast optical switching signals. A typical experiment setup is depicted in Fig. 3. Two laser pulses (either from the same pulse laser or from two different pulse lasers) are usually used in this experiment. Their parameters, such as the wavelength, pulse duration, pulse repetition, or the energy of pump pulse, can be tuned according to designs. The optical delay line, which is actually a precision positioning stage, is introduced to the pump light path to adjust the optical length difference between the pump and probe laser pulses. The output signals from the prism-film coupling system are detected by a monochromator, amplified by a photomultiplier tube, and finally received by the lock-in amplifier, which is controlled by a computer. There are three lenses in the optical path, which are used to focus the pump light, the input and output probe light that couple with the prism. In addition, except for a beam splitter, many total reflection mirrors are used to reduce the loss of laser energy. By this experimental arrangement, we can measure the linear or nonlinear transmission spectra and the time response with different pump energies for two-dimensional nonlinear photonic crystals. Most of our all-optical switching experiments in two-dimensional nonlinear photonic crystals are performed with this system by only changing the parameters of the incident pump or probe lasers according to our needs.

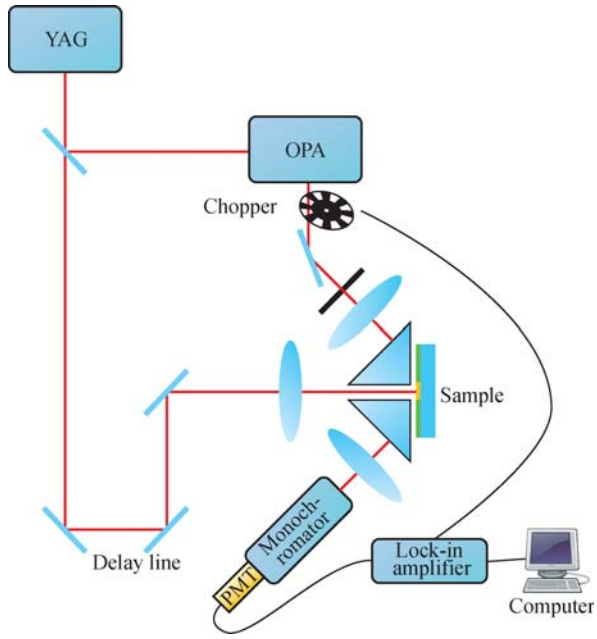

Fig. 3 Schematic configuration of the experiment setup for two-dimensional photonic crystal optical switching.

4.3 Experimental results

Although the physical principle is simple, the experiment operations are still difficult. Here, we will show our main

experimental progress in two-dimensional photonic crystals all-optical switching based on the principles of band gap shift and defect mode shift. The all-optical switching experiments with response time of 10 ps [58] and 20 fs [101] are discussed here.

4.3.1 Optical switching based on the band gap edge shift

In the early stage of our experimental exploration, we adopted the scheme of band gap edge shift to realize optical switching with the response time of 10 ps [58]. Here, we will discuss in detail the experimental design, sample fabrication, measurement process and results of two-dimensional photonic crystal switching based on the band edge shift.

In this experiment, a 1064 nm laser (with a pulse duration and pulse repetition rate of 20 ps and 10 Hz, respectively) from YAG laser (Model PL2143B, Ekspla Ltd., Lithuania) was used as the pump light, while a laser (pulse duration 10 ps and repetition rate 10 Hz) from an optical parameter amplifier (OPA) (Model OPA-740, CAS) with a wavelength range from 450 nm to 650 nm and pumped by the same YAG laser was used as the probe laser. We had performed extensive numerical studies by means of the multiple scattering method [115] and determined that the optimized lattice constant and the radius of the air hole are 220 and 90 nm, respectively. The polystyrene photonic crystal sample was fabricated by using the FIB microfabrication method as mentioned above, and its scanning electron micrograph (SEM) image is shown in Fig. 4. The photonic crystal has a square lattice geometry.

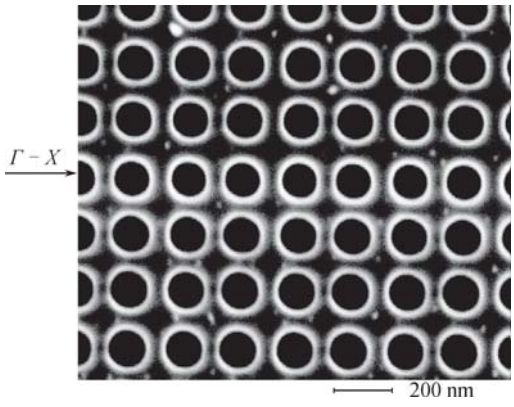

Fig. 4 SEM image of a typical two-dimensional polystyrene photonic crystal made from drilling air holes in polystyrene thin film deposited on a silica substrate.

With the sample at hand, the subsequent experimental measurement process was arranged as follows. First, we measured the linear transmission spectrum of the photonic crystal. The result is shown in Fig. 5, from which we can find that due to the good quality of the periodical lattice of air holes, the gap edge is very steep, a feature that is very suitable for all-optical switching. Then the nonlinear interaction was detected by the experimental setup depicted in Fig. 3. The probe laser was incident along the Γ–X direction of the two-dimensional photonic crystal by the prism coupling technique, while the pump laser was incident normally to the upper surface plane of the photonic crystal. Before measurement, the approximate synchronal position where the optical path difference is almost zero should be found and recorded as a reference point. Then the delay line was tuned by an automatic controller to change the time delay between the pump and probe light. By careful measurement, the transmittance changes of the probe light with respect to the time delay under the pump-probe method were recorded, and the result is shown in Fig. 6.

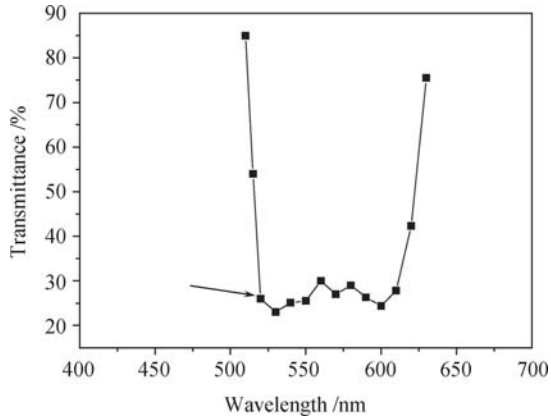

Fig. 5 Measured transmission spectrum of polystyrene photonic crystal. The arrow denotes the spectral position of the probe light.

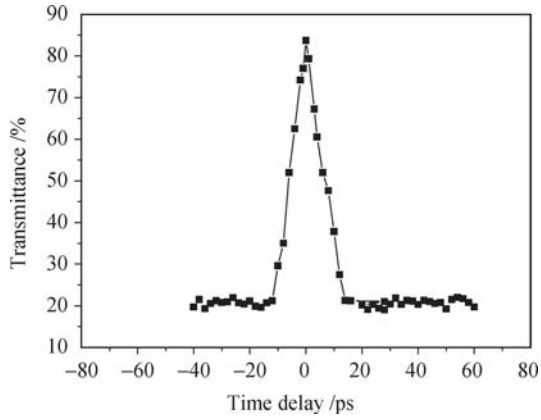

Fig. 6 Measured time delay curve that characterizes the optical switching response of the polystyrene photonic crystal. The peak intensity of the pump laser is 16.7 GW/cm^2. The signal light corresponds to the short wavelength band edge of 519 nm.

Figure 6 clearly reveals the optical switching effect taking place on the polystyrene photonic crystal under external pulse laser pump. Because of the positive third-order nonlinear susceptibility of the polystyrene material, the band gap shifts to the long wavelength direction (red shift). Because the probe signal is located at the short-wavelength band edge, the probe light transmittance will increase and thus a peak appears in the time delay curve. The transmission contrast of the "off"

and "on" states is about 65% under the pump intensity of 16.7 GW/cm^2. The maximum transmission with the transmissivity of 85% is achieved when the pump and probe pulses are of zero time delay and overlap completely in the temporal domain, which corresponds to the "on" state. The minimal transmission with the transmissivity of 20% happens when the two pulses are far away from synchronization, which is in the "off" state of optical switching. On the other hand, we can measure the response time of the optical switching from the full width at half maximum (FWHM) of the time delay curve, which is around 20 ps according to Fig. 6. The response time is close to the pulse duration of the pump light. This indicates that the optical switching response time of the nonlinear photonic crystal is limited by the experimental time resolution, such as the duration of pump pulse. This method of extracting the time response was previously used by Shimizu and Ishihara [116].

To better understand the optical switching properties, the dynamical shift of the photonic band gap was also studied. We measured the shift of the two photonic band gap edges which correspond to the probe wavelength of 519 and 627 nm, respectively. The results are shown in Fig. 7, from which we can find that the long wavelength band edge shifts notably more than the short wavelength band edge. This behavior can be understood from the basic knowledge about photonic band structures. According to this theory, the low-frequency modes at the dielectric band mainly concentrate their energy in the high-dielectric constant regions, while the high-frequency modes at the air band mainly concentrate their energy in the low-dielectric constant regions [3]. In our photonic crystal structure, the nonlinear material has the high-dielectric constant, and its refractive index changes with the pump pulse. As a result, the pump light will affect more the refractive index of polystyrene when it excites the low-frequency modes than when it excites the high-frequency modes. Therefore, the long-wavelength band gap edge will shift by a larger quantity. The simulation results of band gap shift at the long and short wavelength band edge are also shown in Fig. 7 (*lines*). Good agreement is achieved between theory and experiment.

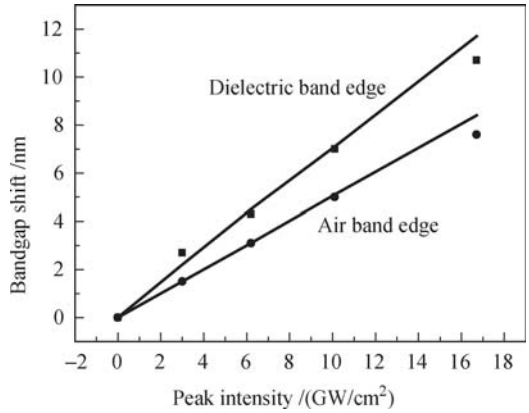

Fig. 7 Measured (*symbols*) and calculated (*lines*) shift of the photonic band gap edges with different pump intensities. Both the short and long wavelength band edges are examined.

Polystyrene, as an organic conjugated polymer, possesses a relatively large third-order nonlinear susceptibility and very fast (down to a few femtoseconds, almost instantaneously) response time. From the above analysis, the optical switching response time of the nonlinear photonic crystal is mainly limited by the time resolution of experimental measurements, which is largely determined by the duration of the pump pulse. So if the pump and probe pulse is significantly shortened down to the femtosecond scale, the femtosecond response time of all-optical switching may be achieved.

Based on this consideration, a homemade Ti:sapphire laser (TFS-1, Institute of Physics, Chinese Academy of Sciences) with a pulse duration and pulse repetition rate of 25 fs and 80 MHz was used as the incident probe and pump pulse. Because the central wavelength of the Ti:sapphire laser is located at around 800 nm, the optimized lattice constant and the hole radius were found via numerical simulation to be 350 and 115 nm, respectively, for which the band gap of the photonic crystal is near 800 nm [101]. The SEM image and measured linear

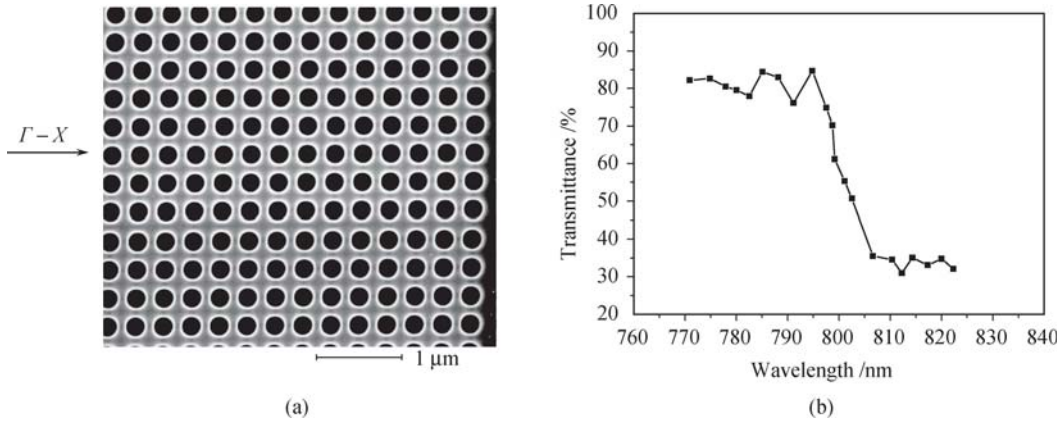

Fig. 8 **(a)** SEM image of the photonic crystal and **(b)** measured linear transmission spectrum, which indicates the band gap edge located at about 800 nm.

transmission spectrum of this photonic crystal is shown in Fig. 8.

In the current experiment to characterize the optical switching properties, the pump and probe lights have the same wavelength. The experimental setup is similar to that shown in Fig. 3 except that the OPA system is replaced by a total reflection mirror, and a beam splitter with an intensity ratio of 1:9 was used to separate the incident laser pulse into the pump and probe pulses. The pump light had an intensity of about 13 GW/cm^2. In the experiment, the probe light was selected to have a wavelength of 806 nm, which is located at the short-wavelength band edge of the photonic crystal. The synchronization of the two femtosecond pulses with the duration of 25 fs was also needed before recording the experimental data. For this aim, a finer stage was used in the arm of optical delay line. The measured time delay curve of optical switching signals is shown in Fig. 9. The all-optical switching of the polystyrene photonic crystal has reached an ultrafast response time of 20 fs, which is measured from the FWHM of the time delay curve. The transmittance contrast is from 33% to 78% when the system changes from the "off" state to the "on" state.

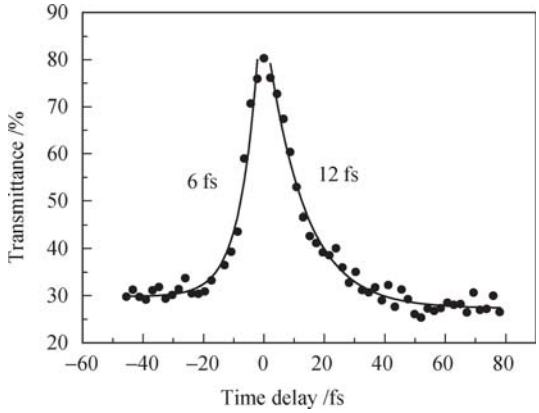

Fig. 9 Measured transmittance change depending on the time delay between pump and probe beam. The solid lines represent the exponential fits of the experimental points.

The above optical switching is based on the principle of the band gap edge shift. The performance of the devices will be largely influenced by the quality of the photonic crystal samples. If the periodicity is very good, the band gap edge will be very steep, which in turn will make a larger switching contrast under the same or even lower pump power. Generally speaking, a defect mode will provide a steeper edge than the band gap edge in the photonic crystal system due to its fine resonance nature. For this reason, in our works we also paid much attention to all-optical switching based on the defect mode shift in nonlinear photonic crystals.

4.3.2 Optical switching based on the defect mode shift

In this part, we will show the all-optical switching with the response time of 10 ps in a two-dimensional polystyrene photonic crystal with a defect [100]. In this experiment, the 1064 nm laser (with a pulse duration and pulse repetition rate of 20 ps and 10 Hz, respectively) from YAG laser (Model PL2143B, Ekspla Ltd., Lithuania) was used as the pump light, while a laser (pulse duration 10 ps and repetition rate 10 Hz) from an OPA (Model OPA-740, CAS) with a wavelength range from 450 nm to 650 nm and pumped by the same YAG laser was used as the probe laser. What we needed to do first is to design a structure whose defect mode is located at the wavelength range of the OPA laser. The SEM image of the fabricated polystyrene photonic crystal is shown in Fig. 10. The crystal has a square-lattice structure, with the lattice constant and radius of the air hole being 220 nm and 90 nm, respectively. A line defect is introduced right at the center of the sample, with the width (center-to-center distance between two adjacent rows of air holes) being 310 nm. The patterned area is about 2.5 μm × 100 μm.

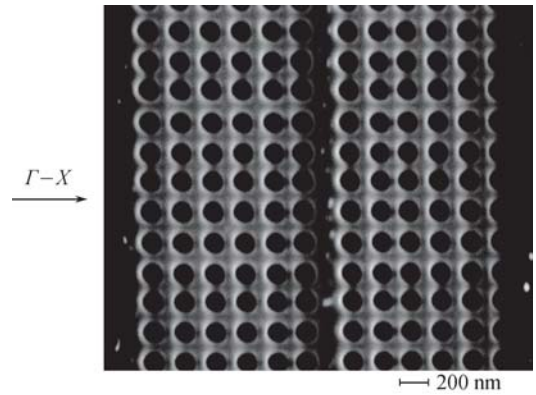

Fig. 10 SEM image of a two-dimensional polystyrene photonic crystal with a line defect located at the center. The lattice constant and the radius of the air hole are 220 and 90 nm, respectively. The width of the line defect is 310 nm.

The measurement method used in this experiment is the same as in the above photonic crystal switching experiments based on the band gap edge shift. The experimental results of the transmission spectrum and time delay curve are shown in Fig. 11. The quality factor of the defect mode is around 140. We find that the response time of the switching is around 10 ps, and the contrast of the "on" and "off" state is about 70% (from 20% to 90%) under the pump intensity of 18.7 GW/cm^2. In addition, the defect mode shifts with different pump intensities were detected and the results are shown in Fig. 12(a). The experimental measurement results agree well with the calculation results obtained by the multiple scattering method, as shown in Fig. 12(b).

So far, we have made a detailed review of our all-optical switching experiments with the response time of 10 ps and 20 fs in two-dimensional polystyrene photonic crystals based on the band gap edge or defect mode shift. Deliberate pump-probe technique in combination with

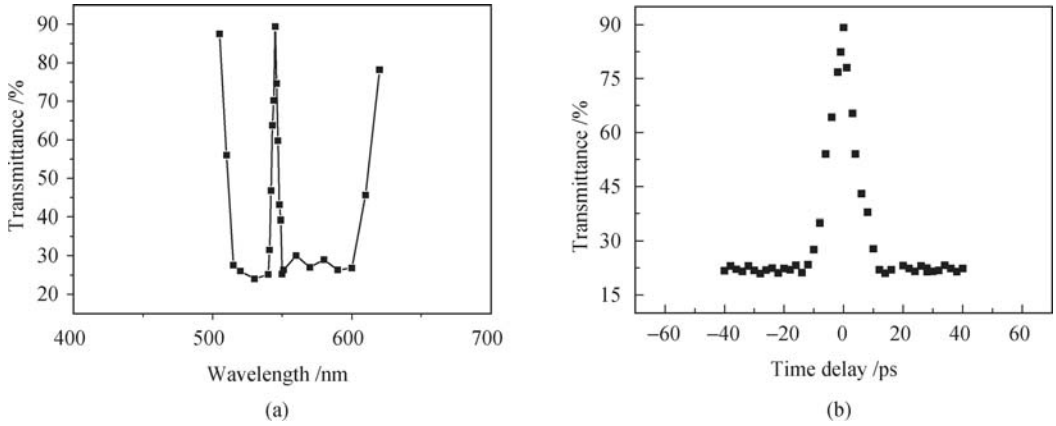

Fig. 11 **(a)** Measured transmission spectrum of the two-dimensional defect photonic crystal shown in Fig. 10. **(b)** Measured transmittance changes of the probe light as a function of the time delay between the pump and probe pulse. The wavelength of the probe light is 545 nm and the pump intensity is 18.7 GW/cm^2.

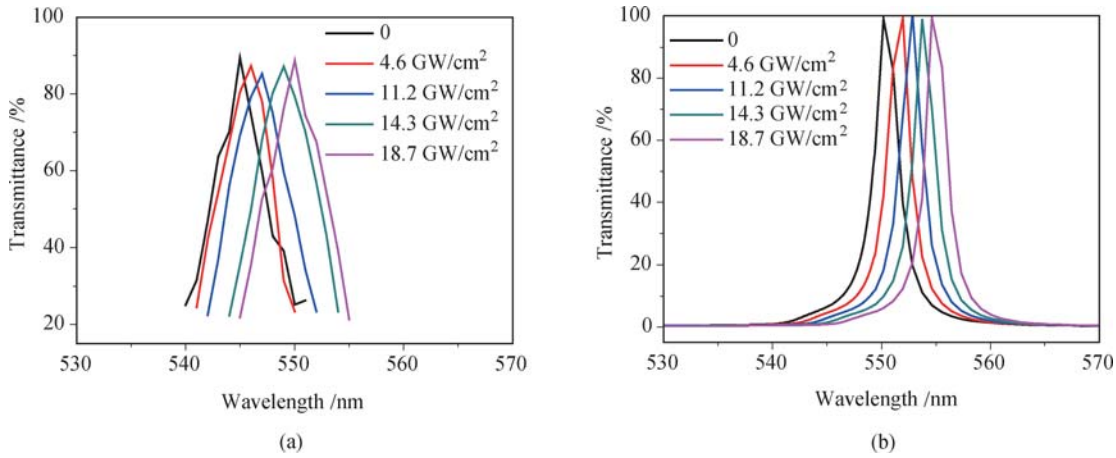

Fig. 12 Shifts of defect mode under different pump intensities. **(a)** Experimental results and **(b)** calculation results.

ultrafast pulse laser technique allows us to characterize the properties and performances of these all-optical switching structures. The realization of these structures heavily relies on state-of-the-art microfabrication technologies, which is rather expensive and size limited. To obtain a large area nonlinear photonic crystal sample with lower expense, we turn to exploit other fabrication methods. One excellent candidate is the self-assembly technique, a chemical approach that allows synthesis of three-dimensional polystyrene opal photonic crystals with good crystalline quality and large area. Extensive experiments have been carried out to characterize the optical switching properties of these three-dimensional nonlinear photonic crystals, which will be discussed in the next section.

5 All-optical switching in three-dimensional nonlinear photonic crystals

Because of the development of state-of-the-art microfabrication technologies, good quality photonic crystal samples can be fabricated readily and most of the studies on the visible photonic crystal are focused on two-dimensional photonic crystals because of the relative ease of fabrication. Nonetheless, extensive efforts have also been made toward visible and infrared three-dimensional photonic crystals continually ever since the concept of photonic crystals was raised. Different methods are diligently exploited to realize three-dimensional photonic crystal structures in the infrared and visible bands. Among them, there are two prominent and efficient schemes: holographic lithography method [117] and self-assembly method [118].

The self-assembly method is easy to operate and is able to grow samples with a large area, so this technique has received more and more attention and many improvements have been introduced. The earlier studies of self-assembly methods include the repulsive electrostatic interactions [119–121], gravitational sedimentation [122], electrophoresis [123], physical limited method [124], templating method [125] and so on. These methods were found to involve obvious disadvantages, such as long preparation time, difficult control of the growth progress, bad crystalline quality, and complex preparation techniques. The vertical deposition method, first

proposed by Jiang and Colvin in 1999 [126], has been proven to be successful for fabricating a high quality three-dimensional opal photonic crystal. Since its proposal, the method has received much attention, and now it has become the widely used method to fabricate three-dimensional photonic crystals.

However, there are still some limitations in the traditional vertical deposition method. First, the growth time is still long, which usually needs several days. Second, many factors in the growth process cannot be controlled efficiently. Third, if the diameter of spheres is too small, such as less than 200 nm, the quality of samples will be affected by Brownian motion. On the other hand, if the diameter of spheres is too large, such as bigger than 600 nm, the spheres will deposit to the bottom of the container by the effect of gravitational settling. To solve the above main problems of the traditional vertical deposition method, several improved methods were proposed, such as the temperature gradient method [127], mechanical agitation method [128], accelerated evaporation method [129], and isothermal heating evaporation-induced self-assembly [130]. These methods have the common characteristics of keeping spheres suspended in the dispersion by convective flows, which can overcome the gravitational settling, and allow for easy control. However, these methods are not very suitable to our polystyrene spheres. Recently, a new self-assembly method called the pressure controlled isothermal heating vertical deposition method (PCIHVD) was developed by Meng's group [131]. The new method is highly effective, easy to control and operate, has good repeatability and is suitable for various sphere diameters. Using this method, a series of high quality polystyrene three-dimensional opal photonic crystal samples has been successfully synthesized. The PCIHVD method has proven to be very suitable for preparation of high quality three-dimensional polystyrene photonic crystal samples. In contrast, our earlier polystyrene opal photonic crystals were prepared by the traditional vertical deposition method and their optical performance was not as good.

5.1 Preparation of three-dimensional polystyrene photonic crystal samples

In this subsection we briefly introduce the PCIHVD method in application to the synthesis of three-dimensional polystyrene nonlinear photonic crystals. The schematic diagram of the synthesis experimental setup is shown in Fig. 13. The vial containing a colloidal suspension consisted of polystyrene spheres and deionized water is immersed in an isothermal deposition bath. A clean glass substrate is fixed in the center of the vial. The vial is sealed and connected to the pressure controlling system. The pressure controlling system is just a vacuum pump connected to the deposition vial with a soft suction pipe. The pressure in the growth chamber is measured using a mercury vacuum gauge. The vacuum pump is started and the pressure is precisely adjusted in the growth chamber with a needle valve. The temperature and the pressure in the deposition vial will become steady in 3 minutes.

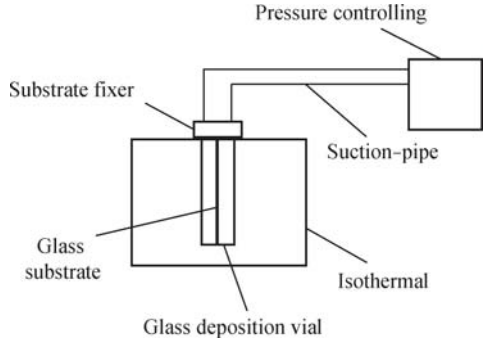

Fig. 13 Schematic of the experimental equipment for PCIHVD method to fabricate three-dimensional opal photonic crystals.

As is known, the critical condition for successful synthesis of opal photonic crystals is that the deposition rate of the spheres is matched with the evaporation rate of the solvent. Because the evaporation rate of the solvent is a function of temperature and the vapor pressure, in order to optimize the sample quality with different diameters of spheres, a variety of conditions with different combinations of temperature and pressure should be experimented, from which we try to find an optimum condition for a certain diameter of spheres. In addition, our experimental results show that the thickness of samples is dependent on the concentration of the suspension. Generally speaking, the samples are thicker when the concentration of suspension is higher. However, there is a saturation phenomenon where the thickness of a sample does not increase obviously any more when the concentration increases. More cracks will appear when the sample becomes thicker, leading to degraded crystalline quality. Therefore, there is also an optimum concentration of the suspension for the polystyrene photonic crystal. We have explored optimized growth conditions for the sphere diameter of 235 nm, 360 nm, 451 nm, 596 nm and 1000 nm, respectively. The SEM images of these samples are shown in Fig. 14(a)–(e). The corresponding transmission spectra are displayed in Fig. 15. The strong attenuation at the band gaps and the steep band gap edge clearly indicate that good periodicity and optical quality have been achieved in these samples.

5.2 Experimental setup for all-optical switching characterization

In this subsection, we present our experimental setup to characterize all-optical switching in our three-dimensional polystyrene opal photonic crystals. The pump-probe technique is also used. The coupling prob-

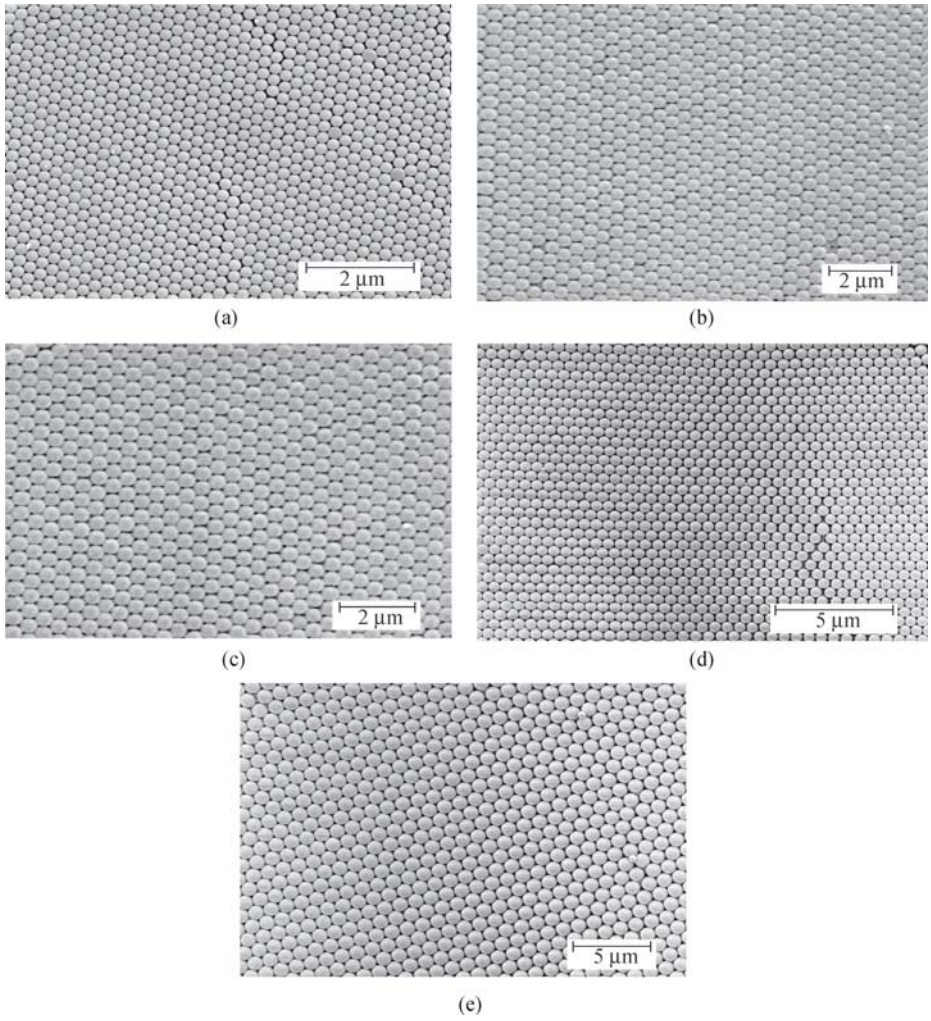

Fig. 14 Top view SEM images of polystyrene photonic crystals synthesized by the PCIHVD method under the optimal growth condition with the sphere diameter of **(a)** 235 nm, **(b)** 360 nm, **(c)** 451 nm, **(d)** 596 nm and **(e)** 1000 nm, respectively.

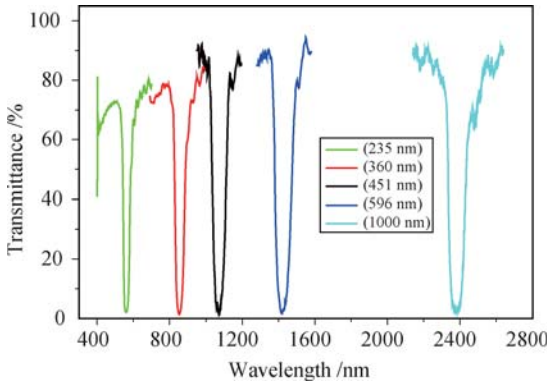

Fig. 15 Measured transmission spectra for the photonic crystals shown in Fig. 14.

lem in these large-area three-dimensional photonic crystal structures is much simpler compared with the situation of two-dimensional photonic crystals. Our samples fabricated by the PCIHVD method has a face-centered cubic structure and its (111) plane is parallel to the surface of the substrate, namely, the Γ–L crystalline direction is perpendicular to the surface. For this reason, we often use the directional band gap of Γ–L for optical switching experiment. Only the scheme of band gap edge shift under the external pump light is considered in this system. As useful defects are difficult to deliberately introduce into the three-dimensional photonic crystal in a controllable and accurate way, the defect mode shift scheme is not exploited for realizing all-optical switching. Although the opal photonic crystal does not have a complete band gap due to low index contrast and structural symmetry, it suffices to only consider a directional band gap for the current purpose. In this regard, the three-dimensional photonic crystal behaves like a one-dimensional photonic crystal, namely, a periodic multilayer distributed Bragg reflector.

The pump or probe laser can be just simply set to be normally incident upon the upper surface of the sample. When the pump and probe beams have the same wavelength, a small angle between the two beams is needed for splitting the beams passing through the sample. Generally, the angle is controlled within 10°. Figure 16a and 16b show the experimental setup when the pump and probe light have different frequencies and when they have the same frequency, respectively.

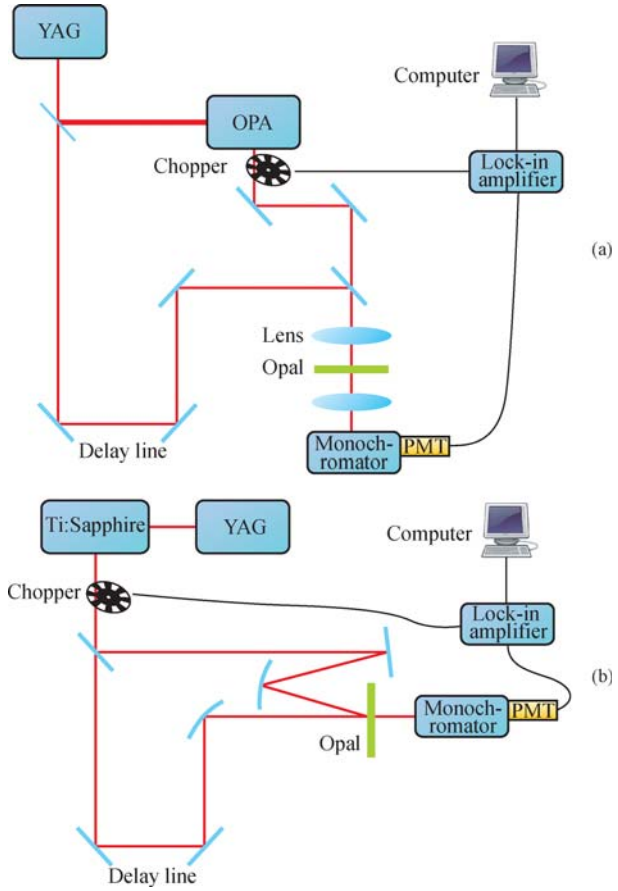

Fig. 16 Experimental setup for characterization of optical switching in three-dimensional polystyrene photonic crystals when the pump and the probe light have **(a)** different frequencies and **(b)** the same frequency.

5.3 Experimental results

In this subsection, we discuss our all-optical switching experiments in three-dimensional polystyrene photonic crystals in detail. The all-optical switches with the response speed of 10 ps [99], 120 fs [96] and 10 fs [102] are presented.

5.3.1 Optical switching with the response time of 10 ps

This is our first all-optical switching experiment, which was demonstrated in 2003. At that time, the self-assembly growth technique of three-dimensional polystyrene photonic crystals was not very good. Figure 17 shows the measured transmission spectrum of our best sample with the sphere diameter of 220 nm.

We measured the optical switching signal with the experimental setup shown in Fig. 16(a). The 1064 nm beam (with the pulse duration and pulse repetition rate of 35 ps and 10 Hz, respectively) from a YAG laser (Model 571-C-10, Continuum, CA, USA) was used as the pump light. The beam (pulse duration 35 ps and repetition rate 10 Hz) from an OPA (Model OPA-740, CAS, Beijing, China) pumped by the YAG laser was used as the probe light. We measured the transmittance change of the probe light beam as a function of the time delay between pump and probe light at the short-wavelength band gap edge of 540 nm and the long-wavelength band gap edge of 580 nm. The results are shown in Figure 18. Although the results were not very good, which was attributed mainly to the bad quality of the polystyrene sample, the change of transmissivity was still observed. This suggested that we must improve the quality of the opal photonic crystal to a considerable extent in order to observe comprehensible optical switching performance. Great efforts were made toward this end in the subsequent years, and things got much better when the PCIHVD approach was developed [131, 132].

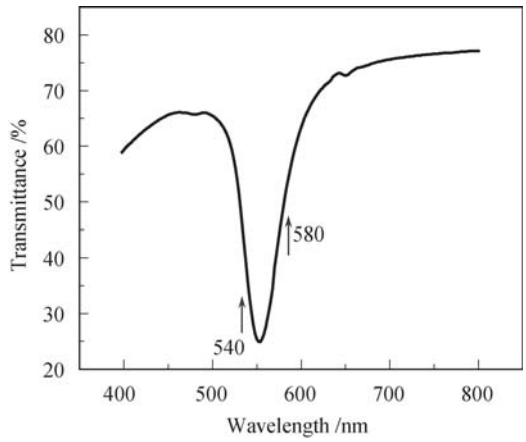

Fig. 17 Measured transmission spectrum of three-dimensional photonic crystal with the sphere diameter of 220 nm.

5.3.2 All-optical switching with the response time of 120 fs

In order to realize more efficient all-optical switching in three-dimensional polystyrene photonic crystals, we managed to improve the quality of samples mainly by means of the PCIHVD synthesis method and designed a much faster optical switching experiment [96]. The natural thing of choice was to introduce the state-of-the-art femtosecond pulse laser technique into our experiment. At that time, a suitable ultrafast pulse laser available was the 800 nm output from a Ti:sapphire laser (TSA-10, Spectra-Physics Co., USA), whose pulse duration and repetition rate are 120 fs and 10 Hz, respectively. The femtosecond laser was used as the pump light. Meanwhile, the tunable output with the pulse duration of 120 fs and repetition rate of 10 Hz from an OPA pumped by the second harmonic of the same Ti:sapphire laser was used as the probe light. The sample with the sphere diameter of 240 nm was prepared by the above PCIHVD method. Very good quality of samples had been achieved according to the SEM images and measured optical transmission spectrum in Fig. 19.

The switching signal was measured with the experi-

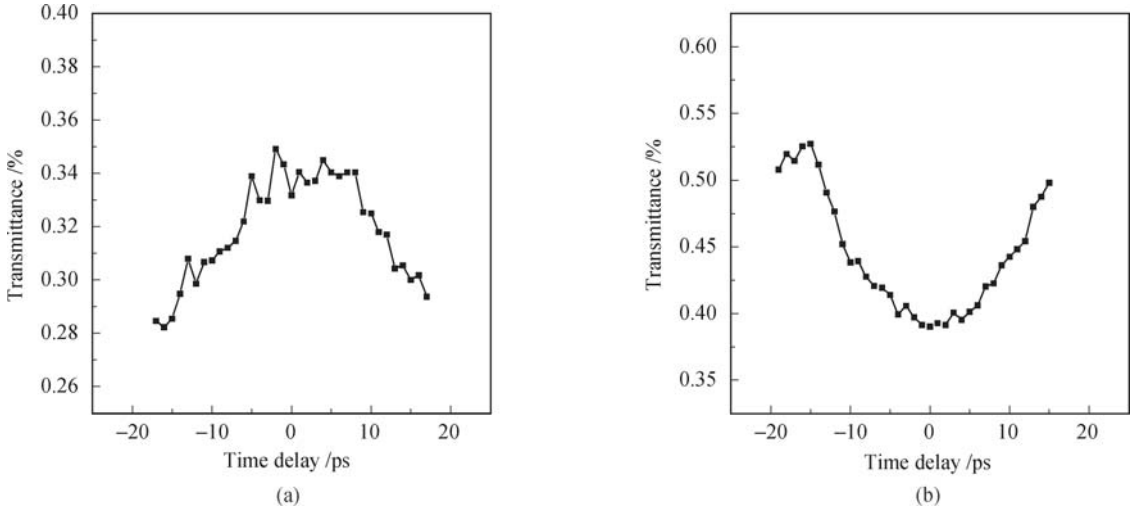

Fig. 18 Experimental results of the transmittance change of probe light with respect to the time delay between the pump and probe light. The probe wavelength and peak intensity of the pump laser are **(a)** 540 nm, 14.4 GW/cm^2 and **(b)** 580 nm, 40.4 GW/cm^2, respectively.

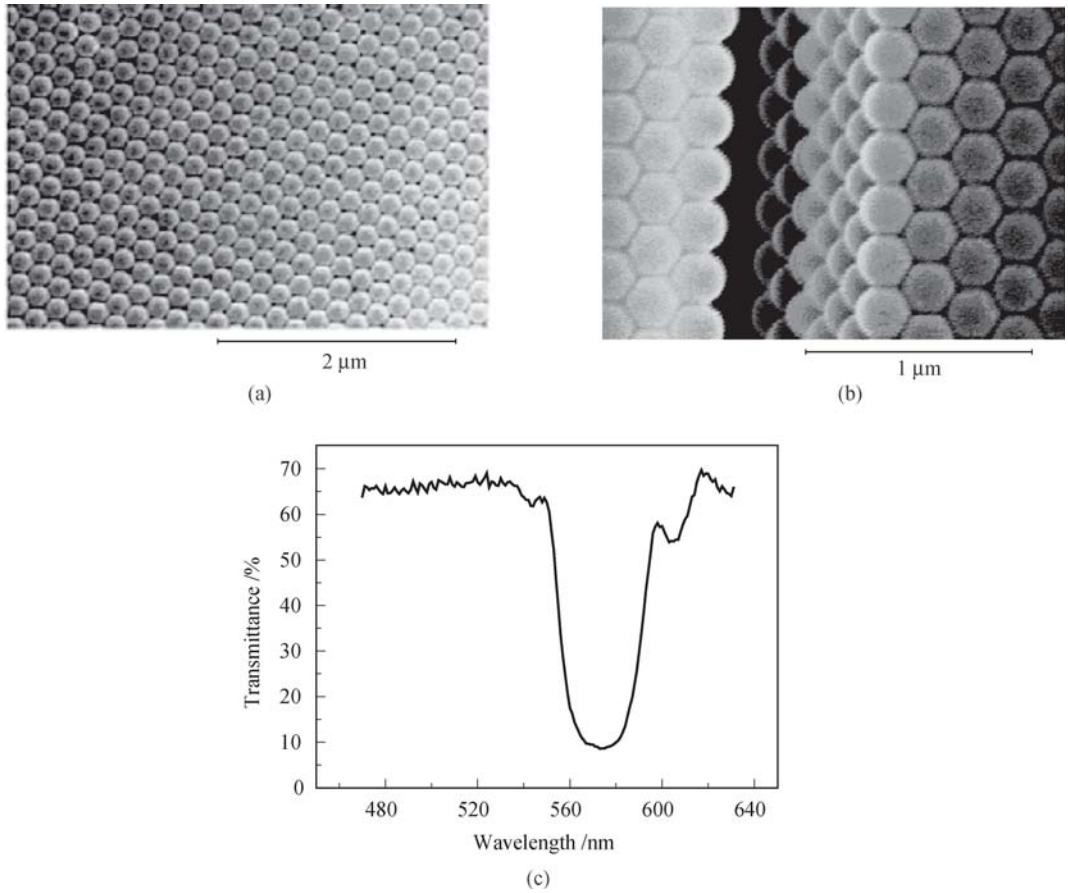

Fig. 19 SEM images and measured transmission spectrum of the polystyrene opal photonic crystal sample with the sphere diameter of 240 nm. **(a)** Surface SEM image, **(b)** cross section SEM image, and **(c)** the transmission spectrum.

ment setup shown in Figure 16a. The probe beam was selected at the short-wavelength band edge of 561 nm. The experimental curve is depicted in Fig. 20. The rising time the optical switching curve is about 120 fs, and the transmissivity jumps from 17% to 62% under the pump intensity of 27.5 GW/cm^2. Basically, the resolved response time of the nonlinear photonic crystal is almost equal to the pulse duration time of the femtosecond laser.

5.3.3 All-optical switching with the response time of 10 fs

In the above experiments, we have shown that the observable response time of the switching with comprehen-

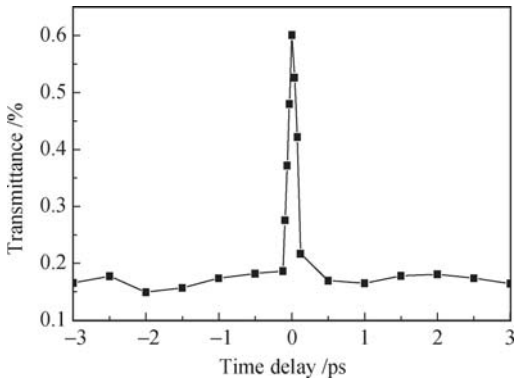

Fig. 20 Measured transmittance of the probe light beam as a function of the time delay between pump and probe pulses. The wavelength of the probe light is 561 nm and the pump intensity is 27.5 GW/cm^2.

sive resolution is almost equal to the pump pulse duration. If the duration of the pump beam becomes shorter, the response time of switching will also become shorter. This is because the response time of switching is determined by the slowest progress of the photonic crystal system. The response time of the polystyrene polymer material was reported to be as short as a few femtoseconds, which means that the material itself is nearly instantaneous in response to external excitation light to change its refractive index under the usual condition of light pulse duration. In order to see to what extent the above simple law of switching response time can be further scaled down to the regime of extremely short light pulse, we proceeded to design a further experiment in the hope of demonstrating all-optical switching with a response time approaching the response time limit of the nonlinear material of polystyrene. The experiment was performed and accomplished in 2007. The result indicated a resolved response time of about 10 fs. To our knowledge, this is the fastest all-optical switching demonstrated in any optical material system.

The ultrafast laser output from a chirped-mirrors Ti:sapphire laser (Horizon-10, CAS, Beijing) with the duration of several femtoseconds was adopted in our experiment. The pulse duration and repetition rate is about 8 fs and 80 MHz, respectively. The Fourier transform spectrum as well as the interferometric autocorrelation signal of the pulse laser is shown in Fig. 21(a) and (b), respectively. The pulse laser covers a very wide spectrum range from 600 nm to 1000 nm with the center located at around 800 nm, indicating a very narrow pulse duration down to two to three laser optical cycles, namely, 6-9 femtoseconds. The autocorrelation signal is more direct to reflect the time-domain properties of the pulse laser. The curve in Fig. 21(b) has a full width at half maximum of about 8 fs, which means that the laser pulse has a duration of about 8 fs.

The three-dimensional sample with a sphere diameter of 360 nm was prepared by the PCIHVD method under optimized synthesis conditions that was particularly designed for this size of sphere. The SEM picture of the synthesized polystyrene opal photonic crystal sample is displayed in Fig. 22(a). The corresponding measured linear transmission spectrum is shown in Fig. 22(b). The central wavelength of the band gap is located at 800 nm. The short-wavelength band gap edge appears steeper than the long-wavelength band gap edge, so the probe beam in this experiment is selected at the wavelength of 785 nm, which is located at the short-wavelength band gap edge.

The experiment setup is shown in Fig. 16(b), due to the same frequency range of pump and probe beams. We should point out that this experiment needs to be under very precise control in order to have comprehensive results. As both the pump and probe beam are ultrafast pulses with the duration of several femtoseconds, the synchronization will be greatly degraded and even disappear when the deflection of the optical path difference is longer than 3 μm. By precise positioning and careful tuning of the optical delay path, as well as hard control of the stability of the femtosecond laser, the time delay curve for optical switching was obtained and

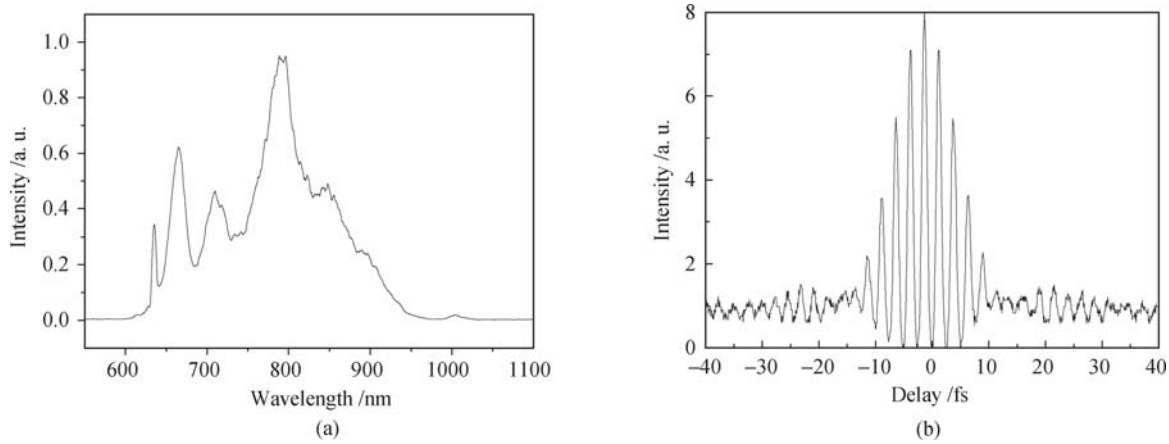

Fig. 21 **(a)** Fourier transform spectrum and **(b)** corresponding interferometric autocorrelation signals of the pump pulse laser beam.

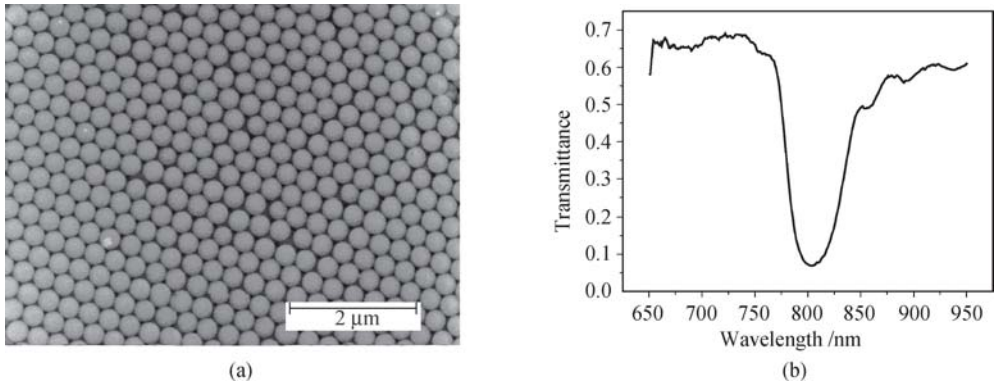

Fig. 22 **(a)** SEM images and **(b)** measured transmission spectrum of the polystyrene opal photonic crystal sample with a sphere diameter of 360 nm.

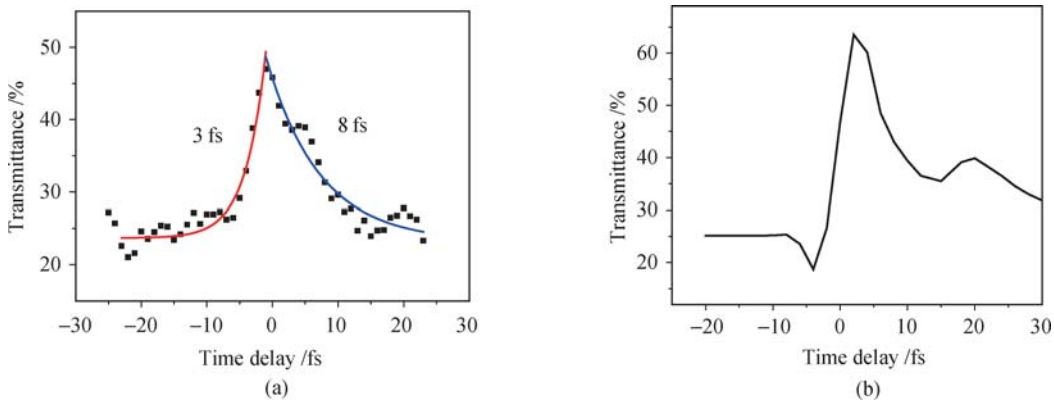

Fig. 23 **(a)** Measured and **(b)** calculated transmittance change with respect to the time delay between pump and probe light. The wavelength of the probe light is 780 nm and the pump intensity is 20.6 GW/cm^2.

is depicted in Fig. 23. From the FWHM of the curve the response time of this all-optical switching is found to be about 10 fs, also close to the pulse duration time. The contrast of transmittance change for this optical switching is only 25% (from 25% to 50%), considerably smaller than the contrast value in the similar three-dimensional sample with much slower response time as 120 fs (shown in Fig. 20), or the contrast value in the two-dimensional sample with similar response time as 20 fs (shown in Fig. 9). Possible reasons for this relatively low contrast of signals include too short pulse duration time, instability of the pulse laser, not steep enough band gap edge, and inaccuracy for determination of the delay path, and so on. It seems that the optical switching response speed for the current nonlinear photonic crystal has been close to its limit set by the finite intrinsic material response time of polystyrene.

6 Efforts to lower pump energy

To evaluate the overall performances of an all-optical switching, one needs to take into account three major parameters, which are threshold power of pump pulse, response time (speed of switching) and switching contrast. So far, all-optical switching with a response time of 10 ps, 20 fs in two-dimensional polystyrene photonic crystals and a response time of 10 ps, 120 fs and 10 fs in three-dimensional polystyrene photonic crystals, have been successfully demonstrated in our previous experiments and have been discussed in great detail. It seems that 10 fs is almost the low limit of response time for these polystyrene structures. Such an optical switching is already several orders of magnitude faster than traditional optical switching based on the scheme of semiconductor two-photon absorption effect. Nonetheless, an ultrafast response speed is not everything for an optical switching that wishes to have practical meanings. Another very important aspect that one needs to consider seriously is to lower the pump intensity to a level that is readily accessible to current practical systems. In our experiments so far, the pump power is in a relatively high level, which is on the order of 10 GW/cm^2. In this section, we will address the problem of how to reduce the pump power in our nonlinear photonic crystal structures.

As is known, for polystyrene material with third-order Kerr nonlinearity, the change of its dielectric constant under strong pump light can be set as: $\Delta\varepsilon = \chi^{(3)}I$. This simple relation implies that two improvements may be used to reduce the pump power. One is to increase the third-order nonlinear optical susceptibility of the Kerr nonlinear material. The other is to design suitable struc-

tures, such as photonic crystal structures with high-Q resonant cavity, to enhance the local field at the areas of nonlinear materials, and this is equivalent to reducing the incident pump power. Many studies have been made along these two feasible routines to realize practically useful ultrafast all-optical switching. In the following we will discuss the recent developments and challenges on this issue.

6.1 Enlarge third-order nonlinear susceptibility of nonlinear materials

In order to enhance the third-order nonlinear susceptibility of nonlinear materials, one can exploit resonant and nonresonant optical processes in the microscopic molecular level. A nonlinear optical process is said to be nonresonant when the wavelengths involved are far from any electronic transitions that directly lead to light absorption. Resonant processes generally have much larger nonlinear susceptibilities, but are slower because real electronic excitations occur. Besides, they also involve considerable absorptive loss of optical energy. Nonresonant processes, as they involve only virtual electronic excitations, are essentially instantaneous, and can avoid attenuation of optical signals [133].

There are two widely used methods to enhance the third-order optical nonlinearity in nonlinear photonic crystals. One way is to harness local field enhancement of surface plasmon resonance (SPR) in the composite system involving tiny metal nanoparticles embedded in the matrix of organic polymer to obtain large third-order optical nonlinearities [134, 135]. The other way is to make use of excited-state induced enhancement of third-order optical susceptibility in π -conjugated molecules [133, 136, 137].

6.1.1 Enhancement by surface plasmon resonance via metal nanoparticles

In recent years, many works have reported the enhancement of third-order nonlinearity in composite systems made from the combination of metal nanoparticles and other nonlinear materials. Structures involving dispersed nanoparticles by spin coating method [138] or shell coated nanoparticles by certain chemical synthesis methods [135] have been observed to have large third-order nonlinear susceptibilities. SPR is a resonant effect that can be fully exploited to enhance the third-order nonlinear susceptibilities. One significant feature of SPR is the enhancement of the electric field near the metal particles, which in turn can enhance many kinds of photoexcitation processes (such as third-order nonlinearity) occurring near the metal particles as long as the photoexcitation and SPR occur at the same wavelength [139]. The shape of metal nanoparticles, dielectric environment, and structure are several important parameters for determining the SPR frequency and the optical nonlinearity properties. A significant challenge for enhancing the optical nonlinear response in materials is controlling the geometric structure of metal nanoparticles and achieving a high particle filling factor in the process of implanting these particles into host matrixes.

Because SPR is basically a resonant effect, the enhancement effect is somewhat limited to only happen efficiently at the resonant wavelength of metal nanoparticles. Large third-order optical nonlinear responses are observed at the SPR wavelength but decrease dramatically at wavelengths far from the SPR. On the other hand, when SPR takes place, the absorption effect of light is also greatly enlarged, and this will degrade the overall optical performance of nonlinear optical materials. In this regard, an important issue is to design a composite matrix material with large third-order nonlinear susceptibility and simultaneously low linear absorption coefficient.

6.1.2 Enhancement by excited-state introduction

In conjugated organic polymers, such as polystyrene, Garito *et al.* pointed out the possibility of obtaining larger optical nonlinearities by populating polymer molecules on excited states under nonresonant conditions [133, 136]. In a recent work, Hu *et al.* proposed a new strategy to associate the resonant and nonresonant processes together [15]. They fabricated a two-dimensional photonic crystal on the composite matrix made from polystyrene doped with coumarin 153 (C153). The dye molecule C153 absorbs light from the pump beam, which is a resonant excitation, and then transfers its energy directly and efficiently to the polystyrene molecule. The polystyrene molecule exhibits a nonlinear response in a very different wavelength window far from absorption, which is a nonresonant process. In this method, the resonant process provides much larger nonlinear susceptibility, and the absorption of optical signal is avoided due to the nonresonant process. The third-order nonlinear optical susceptibility on the order of 10^{-7} esu has been reached in their composite material. As a comparison, for pure polystyrene material, the third-order nonlinear susceptibility is on the order of 10^{-9} esu.

6.2 Harnessing local field enhancement in resonant nanostructures

The above scheme has been focused on enhancing the nonlinear susceptibility of polystyrene material in the microscopic level of molecules and electrons, namely, to enlarge the quantity of $\chi^{(3)}$ in the formula of $\Delta\varepsilon = \chi^{(3)}I$. Another scheme is to utilize the macroscopic effect of electromagnetic fields to enlarge the local field intensity

at the position of nonlinear materials, namely, the quantity of I in the formula of $\Delta\varepsilon = \chi^{(3)}I$. This scheme has offered more flexibility to achieve this purpose as a wide variety of artificial nanostructures can be designed at will by computer simulations and brought to practice by state-of-the-art microfabrication technologies. An optimized structure with giant local field enhancement can become very important for the realization of low-power all-optical switching. A typical example for this purpose is the high-Q resonant cavity. On the other hand, appropriate optical structures can also be designed to have their optical properties exhibit high sensitivity upon a tiny change of material properties, such as the refractive index. Many interferometric structures belong to this category. In essence, in order to take advantage of the structural flexibility in the macroscopic level, one should manage to find photonic structures that are sensitive to the change of outer optical field. Different devices such as Mach–Zehnder interferometers [140–142], directional couplers [62, 143], ring resonators [7, 144], and photonic crystal cavities [64, 65, 75, 145] have been considered and explored. In the following we will address briefly the principal mechanism of each device that is built on the platform of photonic crystals.

6.2.1 Photonic crystal Mach–Zehnder interferometers

A Mach–Zehnder interferometer with zero path-length difference is shown in Fig. 24. The incident beam is divided into two arms. The relative phase of the two arms will determine the intensity of the output light. The intensity transmitted through the interferometer is a function of the optical frequency and depends on the optical path length difference and the propagation coefficient. If the path length difference is an even multiple of wavelength, the output will be maximum, while if the path length difference is an odd multiple of half-wavelength, the output will be minimum. For a nonlinear Mach–Zehnder interferometer, one of the arms is replaced by a nonlinear optical waveguides. The optical output is modulated by the phase difference between the linear and nonlinear arms caused by nonlinear effects, such as Kerr effect. The transmitted intensity with or without the pump power will be changed.

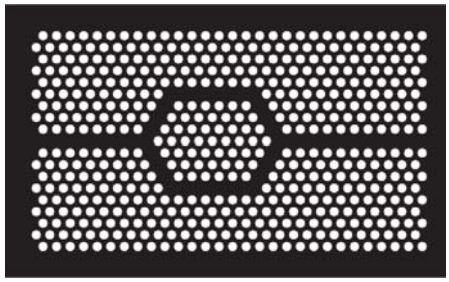

Fig. 24 Schematic diagram of a Mach–Zehnder interferometer in two-dimensional photonic crystals.

Because of the optical interference process of two beams in the Mach–Zehnder interferometer, the output intensity will be very sensitive to small change of phase caused by nonlinearity. By optimization of several geometrical parameters including the lengths of each arm, the lattice, and the radius of air holes, all-optical switching with low pump power can be realized [146]. Notice that this device does not involve significant local field enhancement. The nonlinear effect is amplified by transporting light for a path that is long enough to accumulate sufficient phase shift so that it can be detected. In this regard, it is the interferometric effect of light here that lowers down the pump power.

6.2.2 Photonic crystal directional couplers

The schematic diagram of a photonic crystal directional coupler is shown in Fig. 25, where the two waveguides have Kerr nonlinearity. If the two nonlinear waveguides are close enough to each other, light confined within one of the waveguides can jump to the other after propagating a distance known as coupling length L_c. Suppose that the input is from port 1 and the length of coupling waveguide is an odd multiple of L_c. The output from port 3 will be maximum without Kerr nonlinearity, while the coupling length L_c will change under the pump beam, which will reduce the output from port 3. The change of output intensity from port 3 can be harnessed to serve as all-optical switching. Based on this principle, many studies of all-optical switching have been carried out with low pump power [62, 143]. The key for lowering down the pump power in this device is also the interferometric effect.

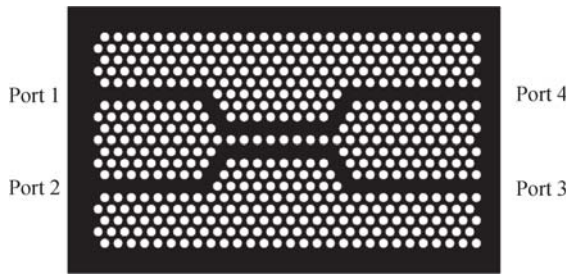

Fig. 25 The schematic diagram of a photonic crystal directional coupler. The signal is input from port 1, and the output signal is detected at port 3, whose intensity sensitively depends on the coupling length in the central region of the device that can be modulated by Kerr nonlinearity.

6.2.3 Photonic crystal high quality factor cavities

In recent years, photonic crystal cavities with a very high quality factor and an ultrasmall modal volume have been demonstrated by the Noda group [147, 148]. Because of the large enhancement of optical nonlinearity and low group velocity achieved by virtue of localized photonic states in defects with high Q factors in photonic crystals,

many nonlinear optical devices such as low threshold optical limiting elements, nonlinear optical diodes and all optical switching can be implemented.

In the usual structures of photonic crystal all-optical switching based on the band edge shift or defect mode shift, the probe beam is often located at the band edge mode or at the defect mode, while the pump beam is often located at the pass band. Here, we will show theoretically that the pump power can be significantly reduced by using a setup where the probe beam is located at the high-Q cavity mode with a very narrow line width. Furthermore, if the central wavelength of the pump pulse is also set to match with this or another high-Q cavity mode, the pump power will be reduced further due to the large field enhancement within the photonic crystal, and more importantly there is no extra prolonged response time of all-optical switching [145].

High-Q cavity modes have very narrow line width in the transmission spectrum and thus exhibit very steep pass band (miniband) edge, which will facilitate low-pump all-optical switching. When the probe beam is located at the high-Q cavity mode, it is very sensitive to the change of refractive index due to the very narrow line width of the cavity mode, and very high switching contrast will be obtained due to the steep band edge. We have made numerical simulations on all-optical switching in a simple one-dimensional nonlinear photonic crystal structure with a resonant cavity of different quality factors of the cavity mode. Here the probe light is matched with the cavity mode, while the pump beam is located at the conduction band. The threshold pump power that is needed to cause a sufficiently large Kerr nonlinearity and refractive index change of polystyrene so that the switching contrast above 95% is determined. The results are summarized in Table 1. It can be found that the pump power can be efficiently reduced with the increase of the cavity mode quality factor, following approximately an inverse proportional law. On the other hand, due to the increasing lifetime of cavities, the switching time is prolonged. The pump power is as low as 63 MW/cm^2 for the probe beam with the quality factor of about 2×10^5, which is three orders of magnitude lower than the pump-power with the quality factor of 331. However, the switching time is 735.27 ps, which is about 470 times longer than the switching time with the quality factor of 331. It seems that compromise needs to be invoked between fast switching speed and low pump power.

The above scheme has been investigated extensively by many groups. Villeneuve *et al.* theoretically proposed a tunable single-mode waveguide microcavity in photonic crystals for ultrafast all-optical switching, and the required operation power is as little as 10 pJ [149]. Almeida *et al.* realized an all-optical switching with its time response of 450 ps on a silicon photonic integrated device by employing a strong light-confinement structure of ring resonator to enhance sensitivity to small changes in the refractive index, and the energy of the control light pulse is as low as 40 pJ [150].

Table 1 Calculated results of pump power with different quality factors of cavity mode. The wavelength of the probe beam matches the peak wavelength of the cavity mode, while the central wavelength of the pump beam is set at the pass band of photonic crystal.

Period	Quality factor	Pump power /(GW·cm^{-2})	Switching contrast	Switching time /ps
5	331	70	96.5%	1.55
6	830	39.4	96.8%	2.87
7	2080	17.5	98.2%	7.31
8	5170	4.375	95.1%	19.08
9	12883	1.575	95%	48.98
10	32096	0.7	96%	118.52
11	79909	0.175	96.2%	295.96
12	199158	0.063	95.8%	735.27

Although the life time of high-Q cavity will restrict the response time of all-optical switching when the probe beam is located at the cavity mode frequency, this method can be efficient when the desirable response time is not very fast, which is true in many practical applications. In this case, we find that when the wavelength of the pump beam is also located at the high-Q cavity mode, the pump power can be further reduced.

We have made numerical simulations on this problem also on the above simple one-dimensional nonlinear photonic crystal model structure. In the simulation, the probe light is matched with one cavity mode, while the

Table 2 Consumed pump power under different quality factors of the cavity mode. The wavelengths of both pump and probe beams are located at the same peak wavelength, which matches the resonant wavelength of the cavity mode.

Period	Quality factor	Maximum power enhancement factor	Pump power /(MW·cm^{-2})	Switching contrast	Switching time /ps
5	331	96.88	1200	95%	1.21
6	830	244.65	525	97%	2.95
7	2080	611.3	84	98.7%	7.70
8	5170	1506.92	21	98.5%	19.69
9	12883	3791.35	1.32	95.3%	49.67
10	32096	9166.47	0.21	97%	121.51

pump light is matched with another cavity mode. The calculated pump power that is needed to cause a sufficiently large switching contrast is summarized in Table 2 for different Q factors for the cavity mode resonantly coupled with the pump light. Here the wavelengths of both pump and probe beams are located at the same peak wavelength, which matches the resonant wavelength of the cavity mode. The pump power reduces with increasing the Q factor associated with the pump beam, also approximately in an inverse proportional law. This means that if high-Q cavity modes are designed both for probe and pump light in nonlinear photonic crystal structures, the enhancement will be a multiplication of these two individual effects. This dual scheme is expected to offer an efficient way to realize very low power all-optical switching in nonlinear photonic crystals.

In the above we have analyzed several schemes to enhance Kerr nonlinearity in nonlinear photonic crystals in order to have ultrafast optical switching on a pump power level that is accessible to most general applications in optical information processing. The problem can be attacked from both the microscopic and macroscopic point of view, by either looking for a material with as large as possible Kerr nonlinear susceptibility of microscopic molecules and sufficiently fast response speed to pump light, or by exploring an appropriate macroscopic optical nanostructure that can enhance the effective Kerr nonlinear susceptibility of optical switching device. However, even if many of the above enhancement schemes can be fully exploited, it is still a challenging task to completely overcome the difficulties and solve the problems to realize all-optical switching with nanoscale or microscale sizes and easy to operate and control, largely due to the lack of appropriate materials with high performance Kerr nonlinearity. It seems that a hopeful way for the fundamental purpose is to combine both the microscopic and macroscopic schemes. Without successful all-optical switching devices, the dream of all-optical integrated chips might still be far off for a long time.

7 Summary and perspective

In this review, we have briefly described the experimental progress that we have made in recent years on exploring ultrafast all-optical switching in two-dimensional and three-dimensional polystyrene Kerr nonlinear photonic crystals and our efforts to continually improve the switching speed to the realm of a few femtoseconds. When nonlinear photonic crystals are pumped by an ultrashort optical pulse with high intensity, the refractive index of the composite polystyrene material will change accordingly and almost instantaneously. This induces the ultrafast shift in the band gap edge or defect state resonant frequency, leading to pass or attenuation of a probe light transporting through the sample, based on which all-optical switching can be formed.

To have a comprehensive understanding of the principles of all-optical switching in nonlinear photonic crystals, we have discussed in detail several relevant issues. We have introduced different mechanisms for the realization of all-optical switching and discussed approaches to prepare high-quality nonlinear photonic crystal samples with considerable band gap attenuation and steep band gap edge by means of microfabrication technique and self-assembly technique. We have described the femtosecond pump-probe technique that is used to characterize the overall performance characteristics of all-optical switching such as the response speed, switching signal contrast, and pump power threshold. The development of the state-of-the-art ultrafast pulse laser technique enables us to experimentally explore the ultimate response speed limit and underlying dynamical picture of all-optical switching based on the polystyrene polymer material. The response time has been scaled down continually from 10 ps, 120 fs, 20 fs, and finally to 10 fs. It seems that the response time is approximately equal to the duration time of pump laser pulse, but a few femtoseconds might have been the limit because it has already been approaching the material response time of polystyrene. To bring ultrafast all-optical switching into reality to facilitate practical applications in optical information processing, the pump power must be significantly lowered by several orders of magnitude from the current value. We have discussed different schemes to reduce the pump power threshold of optical switching in nonlinear photonic crystals, such as surface plasmon resonance effect, resonant cavity effect, and optical interferometric effect. The principle is simple: Enlarging the effective Kerr nonlinear response either by looking for good materials with larger Kerr nonlinear susceptibility in microscopic molecules, or by enhancing the intensity of the local field exerting on Kerr nonlinear materials, or by increasing the effective interaction path of light with Kerr nonlinear materials.

These studies have taught us a lot about the fundamental principles and necessary technologies toward the realization of useful ultrafast all-optical switching in the microscale and nanoscale that can be placed into future all-optical integrated chips.

All-optical switching with high contrast, low pump power, and ultrafast speed is the ultimate goal for researchers. Although great progress has been made, there is still a long way to go. Final success should strongly rely on joint efforts from different aspects of science and technology: physics for better working principle, optics for better detection and characterization techniques, chemistry and materials science for exploration and preparation of new and better Kerr nonlinear materials, and nanotechnology for easy and accurate building of

nanoscale and microscale optical-switching devices. Because all-optical switching is an essential component in all-optical networks, the dream for large-scale optical integrated networks and their connection with traditional microelectronic integrated chips, which are promising for revolutionary information processing technology, will not come true without the success of bringing user friendly, easy to control and tiny all-optical switching devices into reality.

Acknowledgements The authors wish to thank Dr. Yuan-hao Liu and Dr. Xiao-yong Hu for assistance and involvement in previous experiments of optical switching characterization, Prof. Baohua Feng, Prof. Zhi-yi Wei, and Prof. Yan-ying Zhao for assistance in using ultrafast pulse laser techniques, and Dr. Zhong-yu Zheng for assistance in preparing three-dimensional polystyrene nonlinear photonic crystal samples. The financial support from the National Natural Science Foundation of China (Grant Nos. 10634080 and 10525419) and the State Key Development Program for Basic Research of China (Grant No. 2007CB613205) is gratefully acknowledged.

References

1. J. D. Joannopoulos, P. R. Villeneuve, and S. H. Fan, Nature, 1997, 386: 143
2. J. Bravo-Abad, A. Rodriguez, P. Bermel, S. G. Johnson, J. D. Joannopoulos, and M. Soljacic, Opt. Express, 2007, 15: 16161
3. J. D. Joannopoulos, S. G. Johnson, J. N. Winn, and R. D. Meade, Photonic Crystals: Molding the Flow of Light, 2nd Ed., Princeton: Princeton University Press, 2008
4. C. Genet and T. W. Ebbesen, Nature, 2007, 445: 39
5. E. Ozbay, Science, 2006, 311: 189
6. S. R. Friberg, Y. Silberberg, M. K. Oliver, M. J. Andrejco, M. A. Saifi, and P. W. Smith, Appl. Phys. Lett., 1987, 51: 1135
7. V. R. Almeida, C. A. Barrios, R. R. Panepucci, and M. Lipson, Nature, 2004, 431: 1081
8. V. R. Almeida and M. Lipson, Opt. Lett., 2004, 29: 2387
9. K. Sasaki and T. Nagamura, J. Appl. Phys., 1998, 83: 2894
10. K. Sasaki and T. Nagamura, Appl. Phys. Lett., 1997, 71: 434
11. J. L. Bredas, C. Adant, P. Tackx, A. Persoons, and B. M. Pierce, Chem. Rev., 1994, 94: 243
12. A. K. Kar, Polym. Advan. Technol., 2000, 11: 553
13. Z. H. Jin, Z. Y. Li, K. Kasatani, and H. Okamoto, J. Lumin., 2007, 122: 427
14. P. Sharma, S. Roy, and C. P. Singh, Thin. Solid. Films, 2005, 477: 42
15. X. Y. Hu, P. Jiang, C. Y. Ding, H. Yang, and Q. H. Gong, Nature Photonics, 2008, 2: 185
16. V. Morandi, F. Marabelli, V. Amendola, M. Meneghetti, and D. Comoretto, Adv. Funct. Mater., 2007, 17: 2779
17. E. Yablonovitch, Phys. Rev. Lett., 1987, 58: 2059
18. S. John, Phys. Rev. Lett., 1987, 58: 2486
19. Y. N. Barabanenkov and M. Y. Barabanenkov, J. Exp. Theor. Phys., 2003, 96: 674
20. C. J. Jin, B. Y. Cheng, B. Y. Man, Z. L. Li, D. Z. Zhang, S. Z. Ban, and B. Sun, Appl. Phys. Lett., 1999, 75: 1848
21. P. Lalanne, Appl. Opt., 1996, 35: 5369
22. Z. Y. Li, Sci. Technol. Adv. Mater., 2005, 6: 837
23. Z. Y. Li and K. M. Ho, Phys. Rev. B, 2003, 68: 245117
24. A. J. Ward and J. B. Pendry, Phys. Rev. B, 1998, 58: 7252
25. R. W. Ziolkowski and M. Tanaka, Opt. Quant. Electron., 1999, 31: 843
26. M. Bayindir, B. Temelkuran, and E. Ozbay, Phys. Rev. Lett., 2000, 84: 2140
27. X. F. Chen, M. P. Jiang, X. M. Shen, Y. Jin, and Z. Y. Huang, Acta Physica Sinica, 2008, 57: 5709
28. L. Florescu, S. John, T. Quang, and R. Z. Wang, Phys. Rev. A, 2004, 69: 013816
29. G. R. Hadley, IEEE Photon. Tech. Lett., 2002, 14: 642
30. F. Monifi, M. Djavid, A. Ghaffari, and M. S. Abrishamian, J. Opt. Soc. Am. B, 2008, 25: 1805
31. M. Okano and S. Noda, Phys. Rev. B, 2004, 70: 125105
32. H. L. Ren, C. Jiang, W. S. Hu, M. Y. Gao, and J. Y. Wang, Opt. Express, 2006, 14: 2446
33. D. J. Ripin, K. Y. Lim, G. S. Petrich, P. R. Villeneuve, S. H. Fan, E. R. Thoen, J. D. Joannopoulos, E. P. Ippen, and L. A. Kolodziejski, J. Lightwave Technol., 1999, 17: 2152
34. Y. Q. Wang, C. J. Jin, S. Z. Han, B. Y. Cheng, and D. Z. Zhang, Jpn. J. Appl. Phys., 2004, 43: 1666
35. M. Fujita, S. Takahashi, Y. Tanaka, T. Asano, and S. Noda, Science, 2005, 308: 1296
36. C. Hermann and O. Hess, J. Opt. Soc. Am. B, 2002, 19: 3013
37. A. F. Koenderink, M. Kafesaki, C. M. Soukoulis, and V. Sandoghdar, J. Opt. Soc. Am. B, 2006, 23: 1196
38. A. F. Koenderink, M. Kafesaki, C. M. Soukoulis, and V. Sandoghdar, Opt. Lett., 2005, 30: 3210
39. J. Li, B. Jia, G. Zhou, and M. Gu, Appl. Phys. Lett., 2007, 91: 254101
40. K. M. Chen, A. W. Sparks, H. C. Luan, D. R. Lim, K. Wada, and L. C. Kimerling, Appl. Phys. Lett., 1999, 75: 3805
41. D. N. Chigrin, A. V. Lavrinenko, D. A. Yarotsky, and S. V. Gaponenko, J. Lightwave Technol., 1999, 17: 2018
42. S. K. Singh, J. P. Pandey, K. B. Thapa, and S. P. Ojha, Progress in Electromagnetics Research, 2007, 70: 53
43. E. Xifre-Perez, L. F. Marsal, J. Ferre-Borrull, and J. Pallares, J. Appl. Phys., 2007, 102: 063111
44. J. Arentoft, T. Sondergaard, M. Kristensen, A. Boltasseva, M. Thorhauge, and L. Frandsen, Electron. Lett., 2002, 38: 274
45. N. Ikeda, Y. Sugimoto, Y. Tanaka, K. Inoue, and K. Asakawa, IEEE J. Sel. Area. Comm., 2005, 23: 1315
46. M. V. Kotlyar, T. Karle, M. D. Settle, L. O'Faolain, and T. F. Krauss, Appl. Phys. Lett., 2004, 84: 3588
47. S. J. McNab, N. Moll, and Y. A. Vlasov, Opt. Express, 2003, 11: 2927
48. L. O'Faolain, X. Yuan, D. McIntyre, S. Thoms, H. Chong, R. M. De la Rue, and T. F. Krauss, Electron. Lett., 2006, 42: 1454
49. T. A. Birks, J. C. Knight, and P. S. Russell, Opt. Lett.,

1997, 22: 961
50. J. C. Knight, Nature, 2003, 424: 847
51. J. C. Knight, T. A. Birks, P. S. Russell, and D. M. Atkin, Opt. Lett., 1996, 21: 1547
52. A. Ortigosa-Blanch, J. C. Knight, W. J. Wadsworth, J. Arriaga, B. J. Mangan, T. A. Birks, and P. S. J. Russell, Opt. Lett., 2000, 25: 1325
53. G. Calo, A. D'Orazio, M. De Sario, L. Mescia, V. Petruzzelli, and F. Prudenzano, IEEE T. Nanotechnol., 2008, 7: 273
54. M. Djavid and M. S. Abrishamian, Opt. Quant. Electron., 2007, 39: 1183
55. Z. X. Qiang, H. J. Yang, L. Chen, H. Q. Pang, Z. Q. Ma, and W. D. Zhou, Appl. Phys. Lett., 2008, 93: 061106
56. A. David, T. Fujii, B. Moran, S. Nakamura, S. P. DenBaars, C. Weisbuch, and H. Benisty, Appl. Phys. Lett., 2006, 88: 133514
57. J. Q. Xi, M. Ojha, J. L. Plawsky, W. N. Gill, J. K. Kim, and E. F. Schubert, Appl. Phys. Lett., 2005, 87: 031111
58. X. Y. Hu, Y. H. Liu, J. Tian, B. Y. Cheng, and D. Z. Zhang, Appl. Phys. Lett., 2005, 86: 121102
59. A. Locatelli, D. Modotto, D. Paloschi, and C. De Angelis, Opt. Commun., 2004, 237: 97
60. H. Oda, K. Inoue, Y. Tanaka, N. Ikeda, Y. Sugimoto, H. Ishikawa, and K. Asakawa, Appl. Phys. Lett., 2007, 90: 231102
61. V. A. Trofimov and E. B. Tereshin, Opt. Spectrosc., 2005, 99: 961
62. N. Yamamoto, T. Ogawa, and K. Komori, Opt. Express, 2006, 14: 1223
63. F. W. Ye, Y. V. Kartashov, V. A. Vysloukh, and L. Torner, Phys. Rev. A, 2008, 78: 013847
64. M. F. Yanik, S. H. Fan, and M. Soljacic, Appl. Phys. Lett., 2003, 83: 2739
65. M. Soljacic, E. Lidorikis, J. D. Joannopoulos, and L. V. Hau, Appl. Phys. Lett., 2005, 86: 171101
66. T. Tanabe, M. Notomi, S. Mitsugi, A. Shinya, and E. Kuramochi, Appl. Phys. Lett., 2005, 87: 151112
67. M. Scalora, J. P. Dowling, C. M. Bowden, and M. J. Bloemer, Phys. Rev. Lett., 1994, 73: 1368
68. P. Tran, Opt. Lett., 1996, 21: 1138
69. P. Tran, Phys. Rev. B, 1995, 52: 10673
70. L. X. Chen and D. Kim, Opt. Commun., 2003, 218: 19
71. T. Hattori, N. Tsurumachi, and H. Nakatsuka, J. Opt. Soc. Am. B, 1997, 14: 348
72. E. Centeno and D. Felbacq, Phys. Rev. B, 2000, 62: R7683
73. I. L. Lyubchanskii, N. N. Dadoenkova, A. E. Zabolotin, Y. P. Lee, and T. Rasing, J. Appl. Phys., 2008, 103: 07B321
74. S. F. Mingaleev, A. E. Miroshnichenko, and Y. S. Kivshar, Opt. Express, 2007, 15: 12380
75. M. Notomi, A. Shinya, S. Mitsugi, G. Kira, E. Kuramochi, and T. Tanabe, Opt. Express, 2005, 13: 2678
76. T. Tanabe, M. Notomi, S. Mitsugi, A. Shinya, and E. Kuramochi, Opt. Lett., 2005, 30: 2575
77. A. M. Yacomotti, F. Raineri, G. Vecchi, P. Monnier, R. Raj, A. Levenson, B. Ben Bakir, C. Seassal, X. Letartre, R. Viktorovitch, L. Di Cioccio, and J. M. Fedeli, Appl. Phys. Lett., 2006, 88: 231107
78. H. B. Sun, S. Matsuo, and H. Misawa, Appl. Phys. Lett., 1999, 74: 786
79. G. H. Ma, S. H. Tang, J. Shen, Z. J. Zhang, and Z. Y. Hua, Opt. Lett., 2004, 29: 1769
80. S. A. Pruzinsky and P. V. Braun, Adv. Funct. Mater., 2005, 15: 1995
81. I. S. Maksymov, L. F. Marsal, and J. Pallares, Opt. Commun., 2007, 269: 137
82. N. Tetreault, H. Miguez, and G. A. Ozin, Adv. Mater., 2004, 16: 1471
83. A. Hache and M. Bourgeois, Appl. Phys. Lett., 2000, 77: 4089
84. T. G. Euser, H. Wei, J. Kalkman, Y. Jun, A. Polman, D. J. Norris, and W. L. Vos, J. Appl. Phys., 2007, 102: 053111
85. G. P. Agrawal, Nonlinear Fiber Optics, 3rd Ed., New York: Academic Press, 2001
86. G. P. Agrawal, Applications of Nonlinear Fiber Optics, New York: Academic Press, 2001
87. P. Petropoulos, T. M. Monro, W. Belardi, K. Furusawa, J. H. Lee, and D. J. Richardson, Opt. Lett., 2001, 26: 1233
88. J. E. Sharping, M. Fiorentino, P. Kumar, and R. S. Windeler, IEEE Photonic. Tech. L., 2002, 14: 77
89. I. S. Nefedov and V. N. Gusyatnikov, J. Opt. A, 2000, 2: 344
90. H. S. Djie, T. Mei, J. Arokiaraj, and D. Nie, J. Appl. Phys., 2004, 96: 3282
91. F. Z. Henari, K. Morgenstern, W. J. Blau, V. A. Karavanskii, and V. S. Dneprovskii, Appl. Phys. Lett., 1995, 67: 323
92. Y. Vlasov, W. M. J. Green, and F. Xia, Nature Photonics, 2008, 2: 242
93. T. Tanabe, K. Nishiguchi, A. Shinya, E. Kuramochi, H. Inokawa, M. Notomi, K. Yamada, T. Tsuchizawa, T. Watanabe, H. Fukuda, H. Shinojima, and S. Itabashi, Appl. Phys. Lett., 2007, 90: 031115
94. S. W. Leonard, J. P. Mondia, H. M. van Driel, O. Toader, S. John, K. Busch, A. Birner, U. Gosele, and V. Lehmann, Phys. Rev. B, 2000, 61: R2389
95. K. Busch and S. John, Phys. Rev. Lett., 1999, 83: 967
96. Y. H. Liu, X. Y. Hu, D. X. Zhang, B. Y. Cheng, D. Z. Zhang, and Q. B. Meng, Appl. Phys. Lett., 2005, 86: 151102
97. K. F. MacDonald, Z. L. Sámson, M. I. Stockman, N. I. Zheludev, Nature Photonics, 2009, 3: 55
98. K. Asakawa, Y. Sugimoto, Y. Watanabe, N. Ozaki, A. Mizutani, Y. Takata, Y. Kitagawa, H. Ishikawa, N. Ikeda, K. Awazu, X. M. Wang, A. Watanabe, S. Nakamura, S. Ohkouchi, K. Inoue, M. Kristensen, O. Sigmund, P. I. Borel, and R. Baets, New J. Phys., 2006, 8: 25687
99. X. Y. Hu, Q. Zhang, Y. H. Liu, B. Y. Cheng, and D. Z. Zhang, Appl. Phys. Lett., 2003, 83: 2518
100. X. Y. Hu, Q. H. Gong, Y. H. Liu, B. Y. Cheng, and D. Z. Zhang, Appl. Phys. Lett., 2005, 87: 231111
101. D. Z. Zhang, Y. L. Liu, J. Tian, S. Feng, D. X. Zhang, and B. Y. Cheng, Proc. of SPIE, 2006, 6353: 635307
102. Y. Liu, F. Qin, Z. Y. Wei, Q. B. Meng, D. Z. Zhang, and Z. Y. Li, Appl. Phys. Lett., 2009, 95: 131116
103. W. W. Flack, D. S. Soong, A. T. Bell, and D. W. Hess, J. Appl. Phys., 1984, 56: 1199

104. F. C. Peiris, S. Lee, U. Bindley, and J. K. Furdyna, J. Appl. Phys., 1998, 84: 5194
105. P. K. Tien, R. Ulrich, and R. J. Martin, Appl. Phys. Lett., 1969, 14: 291
106. W. Kuang, C. Kim, A. Stapleton, and J. D. O'Brien, Opt. Lett., 2002, 27: 1604
107. P. E. Barclay, K. Srinivasan, M. Borselli, and O. Painter, Opt. Lett., 2004, 29: 697
108. K. Srinivasan, P. E. Barclay, M. Borselli, and O. J. Painter, IEEE J. Sel. Area. Comm., 2005, 23: 1321
109. C. Grillet, C. Smith, D. Freeman, S. Madden, B. Luther-Davis, E. C. Magi, D. J. Moss, and B. J. Eggleton, Opt. Express, 2006, 14: 1070
110. D. Taillaert, W. Bogaerts, P. Bienstman, T. F. Krauss, P. Van Daele, I. Moerman, S. Verstuyft, K. De Mesel, and R. Baets, IEEE J. Quantum. Elect., 2002, 38: 949
111. F. Van Laere, G. Roelkens, M. Ayre, J. Schrauwen, D. Taillaert, D. Van Thourhout, T. E. Krauss, and R. Baets, J. Lightwave Technol., 2007, 25: 151
112. T. Shoji, T. Tsuchizawa, T. Watanabe, K. Yamada, and H. Morita, Electron. Lett., 2002, 38: 1669
113. S. Scheerlinck, J. Schrauwen, F. Van Laere, D. Taillaert, D. Van Thourhout, and R. Baets, Opt. Express, 2007, 15: 9625
114. D. Taillaert, F. Van Laere, M. Ayre, W. Bogaerts, D. Van Thourhout, P. Bienstman, and R. Baets, Japanese Journal of Applied Physics, Part 1: Regular Papers Brief Communications & Review Papers, 2006, 45: 6071
115. L. M. Li and Z. Q. Zhang, Phys. Rev. B, 1998, 58: 9587
116. C. E. Reese, A. V. Mikhonin, M. Kamenjicki, A. Tikhonov, and S. A. Asher, J. Am. Chem. Soc., 2004, 126: 1493
117. M. Campbell, D. N. Sharp, M. T. Harrison, R. G. Denning, and A. J. Turberfield, Nature, 2000, 404: 53
118. Y. N. Xia, B. Gates, and Z. Y. Li, Adv. Mater., 2001, 13: 409
119. P. Pieranski, L. Strzelecki, and B. Pansu, Phys. Rev. Lett., 1983, 50: 900
120. E. A. Kamenetzky, L. G. Magliocco, and H. P. Panzer, Science, 1994, 263: 207
121. Y. N. Xia, B. Gates, Y. D. Yin, and Y. Lu, Adv. Mater., 2000, 12: 693
122. J. X. Zhu, M. Li, R. Rogers, W. Meyer, R. H. Ottewill, W. B. Russell, and P. M. Chaikin, Nature, 1997, 387: 883
123. R. C. Hayward, D. A. Saville, and I. A. Aksay, Nature, 2000, 404: 56
124. S. H. Park and Y. N. Xia, Langmuir, 1999, 15: 266
125. A. vanBlaaderen, R. Ruel, and P. Wiltzius, Nature, 1997, 385: 321
126. P. Jiang, J. F. Bertone, K. S. Hwang, and V. L. Colvin, Chem. Mater., 1999, 11: 2132
127. Y. A. Vlasov, X. Z. Bo, J. C. Sturm, and D. J. Norris, Nature, 2001, 414: 289
128. S. M. Yang, H. Miguez, and G. A. Ozin, Adv. Funct. Mater., 2002, 12: 425
129. V. Kitaev and G. A. Ozin, Adv. Mater., 2003, 15: 75
130. S. Wong, V. Kitaev, and G. A. Ozin, J. Am. Chem. Soc., 2003, 125: 15589
131. Z. Y. Zheng, X. Z. Liu, Y. H. Luo, B. Y. Cheng, D. Z. Zhang, Q. B. Meng, and Y. R. Wang, Appl. Phys. Lett., 2007, 90: 051910
132. Z. Y. Zheng, K. Y. Gao, Y. H. Luo, D. M. Li, Q. B. Meng, Y. R. Wang, and D. Z. Zhang, J. Am. Chem. Soc., 2008, 130: 9785
133. D. C. Rodenberger, J. R. Heflin, and A. F. Garito, Nature, 1992, 359: 309
134. S. T. Selvan, T. Hayakawa, M. Nogami, Y. Kobayashi, L. M. Liz-Marzan, Y. Hamanaka, and A. Nakamura, J. Phys. Chem. B, 2002, 106: 10157
135. Y. Yang, M. Nogami, J. L. Shi, H. R. Chen, G. H. Ma, and S. H. Tang, J. Phys. Chem. B, 2005, 109: 4865
136. Q. L. Zhou, J. R. Heflin, K. Y. Wong, O. Zamanikhamiri, and A. F. Garito, Phys. Rev. A, 1991, 43: 1673
137. J. Oberle, G. Jonusauskas, E. Abraham, and C. Rulliere, Chem. Phys. Lett., 1995, 241: 281
138. H. Shen, B. L. Cheng, G. W. Lu, D. Y. Guan, Z. H. Chen, and G. Z. Yang, J. Phys. D: Appl. Phys., 2006, 39: 233
139. A. Nitzan and L. E. Brus, J. Chem. Phys., 1981, 75: 2205
140. T. Fujisawa and M. Koshiba, J. Lightwave Technol., 2006, 24: 617
141. Y. Tanaka, Y. Sugimoto, N. Ikeda, H. Nakamura, K. Kanamoto, K. Asakawa, and K. Inoue, Appl. Phys. Lett., 2005, 86: 141104
142. C. Y. Liu, Physica E, 2008, 40: 2800
143. F. Cuesta-Soto, A. Martinez, J. Garcia, F. Ramos, P. Sanchis, J. Blasco, and J. Marti, Opt. Express, 2004, 12: 161
144. S. Gulde, A. Jebali, and N. Moll, Opt. Express, 2005, 13: 9502
145. Y. Liu, F. Qin, F. Zhou, and Z. Y. Li, J. Appl. Phys., 2009, 106: 083102
146. H. P. Seigneur, M. N. Leuenberger, and W. V. Schoenfeld, J. Appl. Phys., 2008, 104: 014307
147. Y. Akahane, T. Asano, B. S. Song, and S. Noda, Nature, 2003, 425: 944
148. Y. Akahane, T. Asano, B. S. Song, and S. Noda, Opt. Express, 2005, 13: 1202
149. P. R. Villeneuve, D. S. Abrams, S. H. Fan, and J. D. Joannopoulos, Opt. Lett., 1996, 21: 2017
150. V. R. Almeida, C. A. Barrios, R. R. Panepucci, M. Lipson, M. A. Foster, D. G. Ouzounov, and A. L. Gaeta, Opt. Lett., 2004, 29: 2867